Tectonophysics 656 (2015) 74–90

Contents lists available at ScienceDirect

Tectonophysics

journal homepage: www.elsevier.com/locate/tecto

Miocene-to-Quaternary oblique rifting signature in the Western Ross Sea from fault patterns in the McMurdo Volcanic Group, north Victoria Land, Antarctica

Gianluca Vignaroli [a,*], Fabrizio Balsamo [b], Guido Giordano [a], Federico Rossetti [a], Fabrizio Storti [b]

[a] Dipartimento di Scienze, Sezione di Geologia, Università degli Studi di Roma Tre, Largo S.L. Murialdo 1, 00146 Roma, Italy
[b] NEXT — Natural and Experimental Tectonics Research Group, Dipartimento di Fisica e Scienze della Terra "Macedonio Melloni" — Plesso Geologico, Campus Universitario, Parco Area delle Scienze 157/A, 43124 Parma, Italy

ARTICLE INFO

Article history:
Received 7 December 2014
Received in revised form 20 May 2015
Accepted 25 May 2015
Available online 19 June 2015

Keywords:
Dextral fault system
Volcanism
Rifting
North Victoria Land
Antarctica

ABSTRACT

Mt. Overlord and Mt. Melbourne are part of the fossil-to-active eruptive centre belt of the McMurdo Volcanic Group, located along the western shoulder of the West Antarctic Rift System in north Victoria Land (Antarctica). The formation and localisation of these volcanic centres are intimately connected to the regional fault patterns associated with Neogene transtensional stretching in the West Antarctic Rift System. This study reports about 900 structural data of faults and fault-related joints affecting the Miocene–Pliocene deposits of Mt. Overlord and the Plio-Quaternary deposits of Mt. Melbourne. Fault surfaces strike along three main directions (NW–SE, NE–SW, and N–S) with high (>70°) dip angles. The reconstructed fault geometries and kinematics document a NW–SE strike-slip fault system having dextral motion in the Mt. Overlord area, which evolves into a more complex structural architecture characterised by transtensional deformations in the Mt. Melbourne area, where volcanism is still active. The fault array can be reconciled with principal and subordinate deformation structures developed at the termination region of NW–SE intraplate strike-slip fault systems inducing oblique rifting in the West Antarctic Rift System. The structural dataset, integrated with available geochronological constraints, gives rise to a two-step (Miocene-to-Holocene) tectonic scenario in which the spatial migration of the volcanic activity towards the eastern boundary of the Transantarctic Mountains occurred during the evolution of the West Antarctic Rift System.

1. Introduction

Crustal rifting zones represent tectonic-assisted environments where investigating the linkage between magmatism, volcanism, and faulting. Magma ascent and emplacement are intimately related to the magnitude and orientation of crustal stresses controlling the rifting process (e.g. Gudmundsson, 2006) and, thus, magma percolation benefits of major crustal weakness before feeding the volcanism at the surface. Fault networks and associated fracture zones play an important role in providing a pathway for large volumes of crustal magma propagation (e.g. Buck et al., 2006; Gudmundsson, 2011; Rowland et al., 2010). As such, different mechanisms of faulting have been documented to control the distribution and shape of volcanoes and volcano-related structures (e.g., dyke injections and caldera formation), and they include re-activation of pre-existing structural discontinuities (e.g., Acocella et al., 2002; Seebeck et al., 2010), nucleation and propagation of newly-formed segmented faults (e.g., Rowland and Sibson, 2004), and interaction between active (strike-slip and extensional) intersecting fault systems (e.g., Mouslopoulou et al., 2007). The style and pattern of deformation structures involving the volcanic deposits can be used to decipher the tectonic regime encompassing crustal magma accumulation in active rifting zones (e.g. Acocella et al., 2006; Ebinger et al., 1993; Gudmundsson, 2011; Lesti et al., 2008; Macdonald, 1998; Pollard et al., 1983; Rowland et al., 2007; Wright et al., 2006). Moreover, volcanic deposits can be radiometrically dated because of the occurrence of suitable minerals, thus providing temporal constraints to volcanic events relative to regional deformation. These aspects have great importance in case of volcanic deposits outcropping in rifting areas where very few geological constraints are available for unravelling the regional (neo)tectonic regime.

The Ross Sea region (namely the region that encompasses Victoria Land and the Ross Sea; Fig. 1) of East Antarctica provides a key area to study relationships involving magmatism and regional neotectonics. The evolution of the Ross Sea region is dominated by the Mesozoic–Cenozoic development of the West Antarctic Rift System (WARS) and the Transantarctic Mountains rift shoulder during continental breakup of the Gondwana Supercontinent (Fitzgerald, 2002). The WARS provides the unconventional case of an orthogonal Mesozoic wide rift overprinted on the landward side by Cenozoic oblique narrow rifting

* Corresponding author. Tel.: +39 06 57338043; fax: +39 06 57338002.
E-mail address: gianluca.vignaroli@uniroma3.it (G. Vignaroli).

http://dx.doi.org/10.1016/j.tecto.2015.05.027
0040-1951/

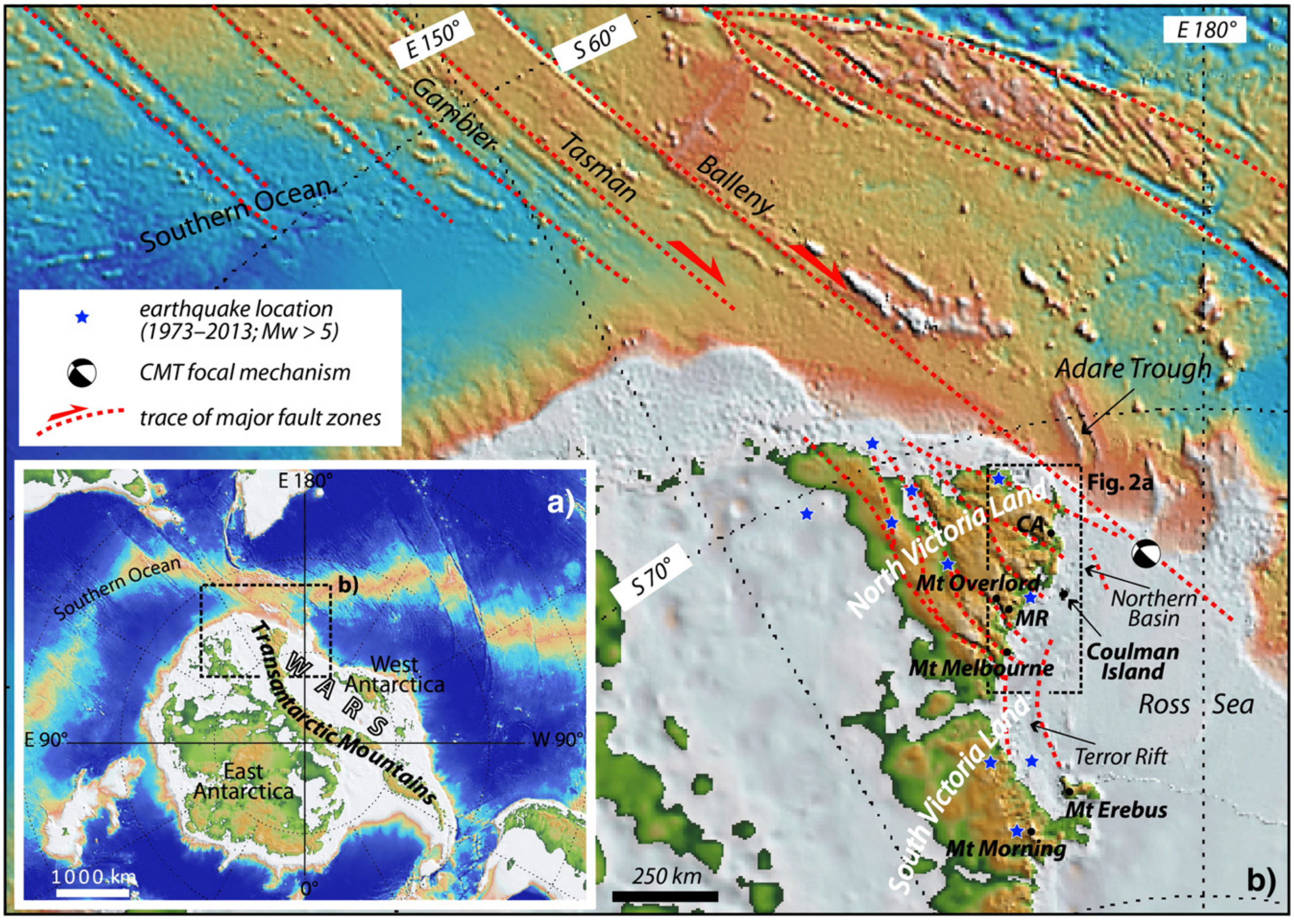

Fig. 1. (a) The Antarctica continent surrounded by the Southern Ocean to the north and the Ross Sea to the east. The trend of the Transantarctic Mountains and the localisation of the West Antarctic Rift System are shown; (b) tectonic map of Victoria Land and surrounding regions showing the trace of major fracture zones and their onshore prolongations. Onshore earthquake localisation and CMT focal mechanism are from Reading (2002) integrated with database extracted from GeoMappApp (http://www.geomapapp.org). The simplified tectonic pattern is from Salvini et al. (1997). Both images have been generated by managing the default basemap from GeoMappApp (Ryan et al., 2009). CA: Cape Adare; and MR: Mount Rittmann.

(Wilson, 1995; Salvini et al., 1997; Hamilton et al., 2001; Rossetti et al., 2006; Storti et al., 2007). This intracontinental rifting is associated with diffuse Tertiary and Quaternary magmatism (e.g., Rocchi et al., 2011; Wörner, 1999). Within this context, regional topography (Faccenna et al., 2008), Neogene-to-Quaternary igneous activity of the McMurdo Volcanic Group (Harrington, 1958; Kyle and Cole, 1974; LeMasurier, 1990; LeMasurier and Thomson, 1990), seismicity (Bannister and Kennett, 2002; Reading, 2002) and GPS data (Dubbini et al., 2010) document neotectonic activity along the coastal region of Victoria Land, facing the Ross Sea embayment. In particular, development of several quiescent-to-active eruptive centres in both north Victoria Land (Mount Melbourne, Mount Overlord, Malta Plateau, Cape Adare, Mount Rittmann) and south Victoria Land (Mount Erebus and Mount Morning) is the most impressive on-shore evidence of present-day tectonics in the region (Fig. 1b).

Still debated are the mechanisms of Cenozoic rifting (orthogonal vs. oblique; e.g. Cande et al., 2000; Müller et al., 2007; Davey et al., 2006; Storti et al., 2007; Di Vincenzo et al., 2013; Granot et al., 2013) as well as the sources and geodynamic scenario for the volcanism in Victoria Land, referred either to a mantle plume (e.g. Behrendt et al., 1991; Hart et al., 1997; Kyle et al., 1992; LeMasurier and Rex, 1991; Storey et al., 1999) or lithospheric-scale strike-slip faulting (Rocchi et al., 2002, 2003; Salvini and Storti, 1999; Salvini et al., 1997). Lanzafame and Villari (1991) first provided a field based dataset for the tectonic structures affecting the Pliocene–Quaternary McMurdo volcanic deposits surrounding the Mt. Melbourne. Since then, volcanic deposits and volcanic-related features have been studied for documenting the neotectonic regimes within the WARS. In south Victoria Land, Martin and Cooper (2010) documented a strike-slip fault system producing dextral offset of a hawaiite dyke dated at 3.88 ± 0.05 Ma. Paulsen and Wilson (2009) reconstructed the Pleistocene stress direction from deformational structures concomitant with volcanism and oblique rifting. In the Admiralty Mountains, Faccenna et al. (2008) found evidence for tectonic control on the emplacement of the Neogene McMurdo Volcanics, which were localised by interference of NW–SE transtensional and NE–SW extensional fault systems in the Cape Adare area (see also Läufer et al., 2006).

This paper deals with the Miocene-to-Quaternary tectonics of the Ross Sea region by presenting the structural pattern (in terms of geometry, spatial distribution, internal architecture, and kinematics) of major fault zones and fault-related joint networks that affect the deposits of the Mt. Overlord and Mt. Melbourne volcanic fields, located in north Victoria Land (Fig. 1b). We performed field mapping and fault-slip analysis along the major fault zones in order to provide new constraints on the tectonic activity post-dating (and/or accompanying) the volcanism in this sector of north Victoria Land. We compare our results with evidence for active tectonics in the whole Victoria Land and we propose WNW–ESE-directed crustal stretching in a context dominated by oblique rifting as the tectonic scenario controlling Miocene–Quaternary volcanism along the western shoulder of the WARS. The structural dataset confirms evidence that tectonics and volcanism, and their space–time evolution, are primary sources of information for constraining the complex geodynamic framework of rifting in the Ross Sea region.

2. Geological outline

North Victoria Land (NVL) occupies an interesting position within the tectonic frame of the Antarctica continent, as (i) it is located at the northern termination of the Transantarctic Mountains, an over 4000-km long orogenic belt that physiographically divides the East Antarctica craton from West Antarctica (Faure and Mensing, 2010), and (ii) it includes the western shoulder of the Mesozoic–Cenozoic WARS, one of the largest intracontinental rift systems on Earth (e.g. Behrendt et al., 1991; Tessensohn and Wörner, 1991; Wörner, 1999) (Fig. 1a).

The geological structure of the Transantarctic Mountains is part of the Gondwana continental pre-breakup paleo-domain (Riley and Knight, 2001). The Transantarctic Mountains consists of Proterozoic to Early Paleozoic basement rocks (e.g., Bomparola et al., 2007; Finn et al., 1999; Flöttmann et al., 1993; GANOVEX Team, 1987; Goodge, 2002; Goodge et al., 2012; Kleinschmidt and Tessensohn, 1987; Rocchi et al., 2011; Rossetti et al., 2011), unconformably overlain by Late Devonian–Triassic sedimentary rocks of the Beacon Supergroup (Collinson et al., 1994). Jurassic intrusive and effusive products of the Ferrar Supergoup (Elliot and Fleming, 2004; Kyle, 1980) complete the regional stratigraphy.

The integration of geological and geophysical datasets has led to a new appreciation of the importance of Cenozoic tectonics in NVL. NW–SE-striking fault systems cut across NVL and run through the northern Ross Sea (Hamilton et al., 2001; Fig. 2a; Salvini et al., 1997), reactivating the Delamerian–Ross orogenic fabric (Di Vincenzo et al., 2013). A dominant Cenozoic dextral strike-slip kinematics, evolving to transtensional in the Ross Sea, has been documented by field data (Capponi et al., 1999; Rossetti et al., 2002, 2003, 2006; Storti et al., 2001, 2006, 2008). The regional pattern of strike-slip and extensional fault systems has been well constrained by seismic profile interpretation (Salvini et al., 1997), magnetic anomaly maps (e.g., Ferraccioli et al., 2000, 2009), and GPS measurements (Dubbini et al., 2010), revealing a complex tectonic framework of crustal-scale NW–SE dextral faults interacting with major N–S-striking extensional faults. This tectonic regime accommodated crustal extension and development of sedimentary basins (e.g., the Adare Trough, the Northern Basin and the Terror Rift) during Cenozoic oblique rifting in the WARS (e.g. Storti et al., 2007). Age of faulting has been provided by dating the deformation structures affecting the basement. ^{40}Ar–^{39}Ar geochronology on (i) kaersutite phenocrysts from syn-tectonic dikes (35–47 Ma; Rocchi et al., 2002), (ii) pseudotachylytes in Paleozoic migmatites (ca. 34 Ma; Di Vincenzo et al., 2004), and (iii) pseudotachylyte-bearing fault rocks in a Cambrian granite (ages younger than ca. 50 Ma; Di Vincenzo et al., 2013) confirm the post-Eocene age for the activation and propagation of intraplate tectonics in basement units of the NVL (Rossetti et al., 2006).

Cenozoic tectonics was closely related with a major period of volcanic activity leading to the formation of one of the most extensive alkaline volcanic provinces in the world: the McMurdo Volcanic Group (Harrington, 1958; Kyle, 1990; LeMasurier and Thomson, 1990). Several works show a correspondence between the fault spatial distribution and the localisation and growth of volcanic edifices of the McMurdo Volcanic Group (Behrendt et al., 1996; Dubbini et al., 2010; Faccenna et al., 2008; Ferraccioli et al., 2009; Rocchi et al., 2003; Salvini and Storti, 1999; Salvini et al., 1997). Within this framework, Mt. Melbourne and Mt. Overlord are large stratovolcanoes located at the intersections between dextral fault systems that cut across the Transantarctic Mountains and the basin-boundary fault systems of the WARS (Fig. 2a). The spatial distribution of some volcanic features (e.g., emergent scoria cones, fumarolic mound alignments, feeder dyke disposition) provides evidence for fault-controlled volcanic activity (Giordano et al., 2012). Lanzafame and Villari (1991) proposed that NW–SE and NNE–SSW striking fault systems control the volcanic setting of the Mt. Melbourne area.

The age of volcanism gradually gets younger moving from Mt. Overlord to Mt. Melbourne. The oldest dated rocks are represented by dolerites exposed at Parasite Cone (north of the Mt. Overlord; ca. 14 Ma), and by lava flows cropping out south of Mt. Overlord (ca. 12–13 Ma; K–Ar whole rock ages; Armienti et al., 1991; Armienti and Baroni, 1999), whereas ages of 7–8 Ma have been reported for the central part of Mt. Overlord (K–Ar whole rock ages; Armienti et al., 1991; Armienti and Baroni, 1999). Pliocene-to-Quaternary ages are reported for the area surrounding the Mt. Melbourne volcano shield (Armienti and Baroni, 1999; Armienti et al., 1991; Giordano et al., 2012). In particular, Giordano et al. (2012) provided ^{40}Ar/^{39}Ar ages on feldspar that separates from both explosive and effusive deposits and reconstructed a four-step, Pliocene-to-Upper Pleistocene time–space evolution of Mt. Melbourne. Middle Pleistocene ages (>400 Ka) are from Mt. Melbourne peripheral centres. These include alkali-basaltic lavas forming dykes and apophyses within the palagonitised lapilli tuffs at Shield Nunatak, Markham Island, and Oscar Point (Fig. 3). The lapilli tuffs are cut by unconformities and syn-eruptive faults and fractures producing local soft-sediment deformation. Younger ages are from the >700 m thick succession exposed at the eruptive centre of Edmonson Point, east of Mt. Melbourne (Fig. 3). Here, a basal trachyte ignimbrite (~90–120 Ka) is overlain by subaqueous-to-subaerial hawaiitic lava cut by dykes that feed sub-horizontal, alkali-basaltic lava flow units having ages younger than 120 Ka. This succession is affected by a series of NE–SW-striking extensional fault zones that produce morphological depressions moving from N to S along the eruptive centre (Giordano et al., 2012). Fumarolic activity at the summit crater (2732 m above sea level) and occurrence of ash layers on ice imply the quiescent state of the Mt. Melbourne volcano.

3. Structural data

The field survey and the structural analysis were aimed at constraining the brittle structural architecture (in terms of spatial distribution, geometry and kinematics of deformation structures) that affects the volcanic deposits exposed in the northern part of the Aviator Glacier, between Forgotten Hills and Eldridge Bluff (hereafter named as the Mt. Overlord area) and in the southern part of the Campbell Glacier, between Baker Rocks and Cape Washington (hereafter named as the Mt. Melbourne area). Field data have been collected in 18 sites (Table 1). Classical field criteria have been used for identifying the kinematic shear sense of fault zones (e.g. Petit, 1987), as well as to classify the fault internal fabrics (e.g. Caine et al., 1996; Gudmundsson et al., 2010) and the fracture pattern (e.g. Atkinson, 1987) in fault damage zones.

The collected structural data are presented by cumulative stereographic projections (Fig. 2). Figure A1 reports stereographic projections for structural data collected at each field site listed in Table 1. Statistical analysis of fault and fracture populations was performed using the software Daisy v.4.1 (Salvini et al., 1999; http://host.uniroma3.it/progetti/fralab). The in-house Monte Carlo-convergent routine was adopted to determine the fault regional kinematic pattern and the orientation of the principal paleo-stress tensors (e.g. Angelier, 1984, 1990) responsible for the generation/re-activation of the considered fault population.

Collectively, 892 structural data of faults and fault-related joints were collected in the two study areas. Cumulative stereographic

Fig. 2. (a) Tectonic map of the north Victoria Land where the study areas are shown (modified and redrawn after GANOVEX Team, 1987; Salvini et al., 1997; Storti et al., 2008); (b–f) cumulative structural data collected in this study for faults (b–d) and joints (e–f) from the two study areas. Data are presented in stereographic projections (Schmidt net, lower hemisphere projection) contouring the fault (b) and joint (e) strike, integrated with polymodal Gaussian distribution statistics of the cumulative fault dip (c), pitch of slickenlines on fault (d), and joint dip (f).

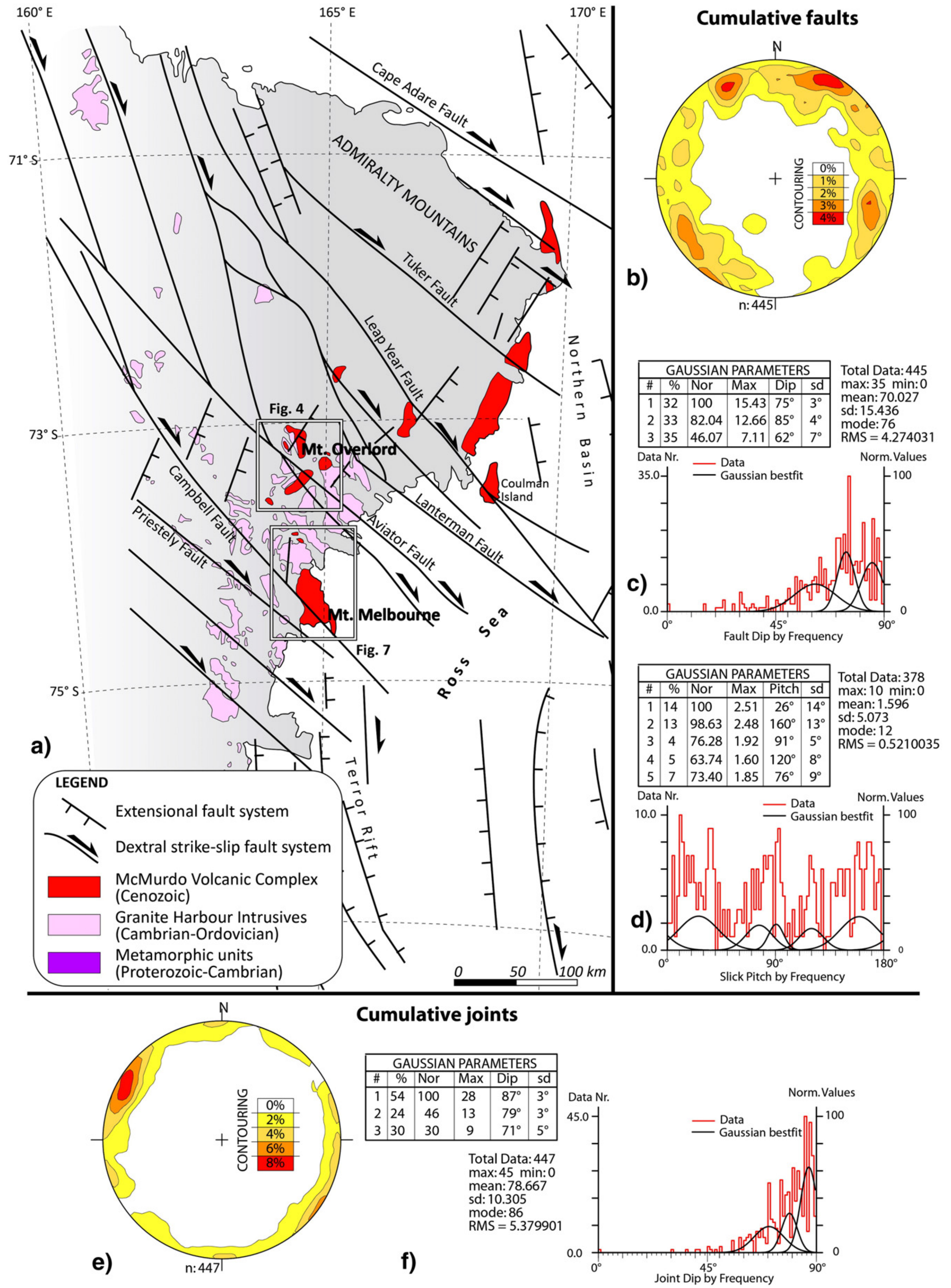

160° E
165° E
170° E
71° S
73° S
75° S
Cape Adare Fault
ADMIRALTY MOUNTAINS
Tuker Fault
Leap Year Fault
Fig. 4
Mt. Overlord
Coulman Island
Northern Basin
Lanterman Fault
Aviator Fault
Campbell Fault
Priestely Fault
Mt. Melbourne
Fig. 7
Ross Sea
Terror Rift
a)
LEGEND
Extensional fault system
Dextral strike-slip fault system
McMurdo Volcanic Complex (Cenozoic)
Granite Harbour Intrusives (Cambrian-Ordovician)
Metamorphic units (Proterozoic-Cambrian)
0 50 100 km
Cumulative faults
N
CONTOURING
0%
1%
2%
3%
4%
b)
n: 445
GAUSSIAN PARAMETERS
% Nor Max Dip sd
1 32 100 15.43 75° 3°
2 33 82.04 12.66 85° 4°
3 35 46.07 7.11 62° 7°
Total Data: 445
max: 35 min: 0
mean: 70.027
sd: 15.436
mode: 76
RMS = 4.274031
Data Nr.
Norm. Values
Data
Gaussian bestfit
35.0
100
0.0
0
0°
45°
90°
c)
Fault Dip by Frequency
GAUSSIAN PARAMETERS
% Nor Max Pitch sd
1 14 100 2.51 26° 14°
2 13 98.63 2.48 160° 13°
3 4 76.28 1.92 91° 5°
4 5 63.74 1.60 120° 8°
5 7 73.40 1.85 76° 9°
Total Data: 378
max: 10 min: 0
mean: 1.596
sd: 5.073
mode: 12
RMS = 0.5210035
Data Nr.
Norm. Values
Data
Gaussian bestfit
10.0
100
0.0
0
0°
90°
180°
d)
Slick Pitch by Frequency
Cumulative joints
N
CONTOURING
0%
2%
4%
6%
8%
e)
n: 447
GAUSSIAN PARAMETERS
% Nor Max Dip sd
1 54 100 28 87° 3°
2 24 46 13 79° 3°
3 30 30 9 71° 5°
Total Data: 447
max: 45 min: 0
mean: 78.667
sd: 10.305
mode: 86
RMS = 5.379901
f)
Data Nr.
Norm. Values
Data
Gaussian bestfit
45.0
100
0.0
0
0°
45°
90°
Joint Dip by Frequency

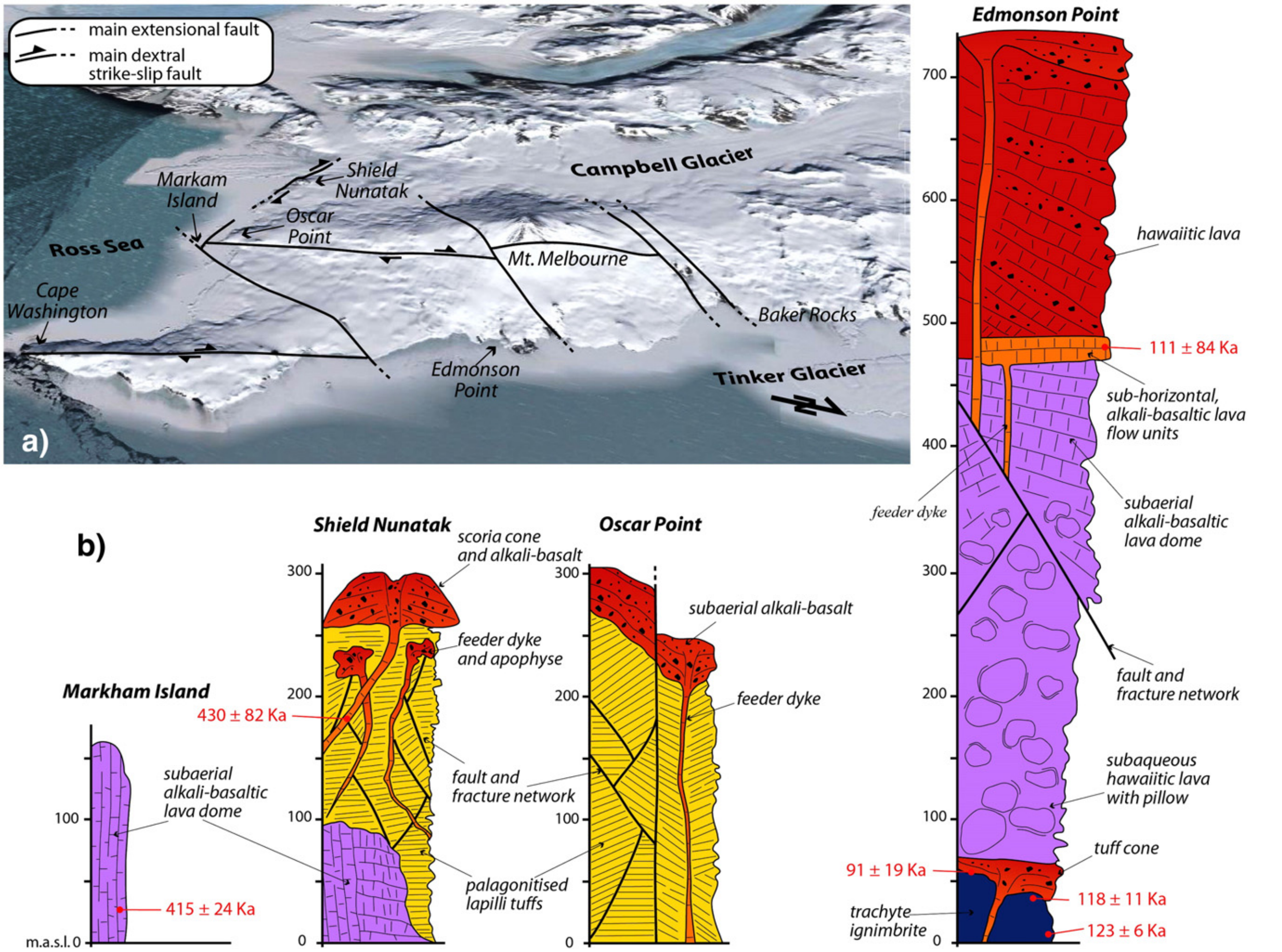

Fig. 3. (a) Google Earth view of the Mt. Melbourne volcanic field; (b) schematic stratigraphies of the volcanic sequences of the Mt. Melbourne, exposed at Markham Island, Shield Nunatak, Oscar Point and Edmonson Point. Ages are from Giordano et al. (2012).

projections show that fault surfaces strike along three main directions: NW–SE, NE–SW, and N–S (mean attitudes: N118°, 82°; N63°, 76°; and N195°, 70°, respectively; Fig. 2b). High to sub-vertical dip values prevail for fault zones (means of 75°, 85°, 62°; Fig. 2c). Five pitch populations (26°, 76°, 91°, 120°, 160°) have been found for measured slickenlines on fault surfaces (Fig. 2d), documenting dominant strike-slip and subordinate dip-slip kinematics. Contouring of pole-to-plane and slick for extensional, reverse, dextral, and sinistral fault sets detected in the study areas are reported in Figure A2. Fault-related joint attitudes cluster along a dominant NNE–SSW direction (Fig. 2e) and high dip values (means of 87°, 79°, 71°; Fig. 2f).

3.1. Mt. Overlord area

In the Mt. Overlord area, the McMurdo volcanic rocks lie on top of granitoid and metamorphic rocks and morphologically define NW–SE aligned ridges (Fig. 4). Major fault zones are aligned along these ridges and probably control the morphological features in the area, such as the steep cliffs of the Aviator Glacier and the tapered shape of the Navigator Nunatak. The most recurrent structural feature in the studied outcrops is a set of NW–SE striking fault zones with strike-slip kinematics and a related joint network (see stereoplots in Fig. 4), producing centimetre-to-metre along-fault offsets of the volcanic deposits. The geometrical architecture of the NW–SE striking fault zones is often complicated by the occurrence of subsidiary fault sets striking at high-angle with respect to the NW–SE ones. These subsidiary faults are both strike-slip and dip-slip faults, with associated joint networks.

NW–SE fault zones are characterised by the alignment of sub-parallel fault segments (Fig. 5a–c) producing up-to one metre thick damaged zones. The length of these faults is over hundred metres. Fault surfaces have general high dip values (>50°), dipping both to NE and SW. In cross section, NW–SE fault zones typically have curvilinear surfaces, resembling flower structures (sites n° 92 and 5; Fig. 5a and c), but sub-planar parallel surfaces also occur (site n° 4; Fig. 5b). Slickenlines on fault surface commonly consist of abrasion striae (Fig. 5d), with pitch values generally less than 30° or more than 150°, indicative of oblique-to-strike-slip kinematics. In plan view, the fault fabric shows a composite architecture (Fig. 6a–f), including millimetre-thick principal slip surfaces having sub-planar geometry, breccias and secondary fractures (site n° 92 and 3). Well-developed fault zones are characterised by cohesive breccia with pronounced grain size reduction (protocataclasite to cataclasite; Fig. 6c) that, in places, is altered by clay minerals (see inset in Fig. 6c). The thickness of the fault cores ranges between about few millimetres (along main slip surfaces; Fig. 6a) to about twenty centimetres (in cohesive breccias and gouges; Fig. 6c). Both fault core and damage zone are characterised by the occurrence of sigmoidal lithons and secondary fractures. The latter consist of synthetic shear surfaces (Riedel shears in Fig. 6c–f) and joints (mode I of Atkinson, 1987; Fig. 6e, f), providing shear criteria of dextral strike-slip movement.

Subsidiary fault sets mostly include ~N–S-striking extensional, subordinate WNW–ESE and NE–SW-striking reverse, and NNE–SSW to NE–SW-striking sinistral strike-slip fault zones (Fig. 4). They are characterised by plurimetric spacing and appear as isolated deformation

Table 1
List of sites of structural measurement.

Study area	Site	n°	Long.	Lat.	El. (m)
Mt. Overlord	Navigator Nunatak	3	S 73°16′03″	E 164°13′23″	1847
	Aviator Gl.–CoPilot Gl.	4	S 73°10′39″	E 164°20′19″	1814
	Mt. Noice	5	S 73°17′41″	E 164°33′39″	1749
	Forgotten Hills	92	S 73°00′05″	E 163°58′14″	2036
	Parasite Cone	93	S 73°05′43″	E 164°17′35″	2106
	Mt. Overlord (south)	94	S 73°12′46″	E 164°26′59″	2495
	Eldridge Bluff	97	S 73°24′38″	E 164°40′49″	751
	Mt. Noice	109	S 73°17′19″	E 164°39′39″	2510
Mt. Melbourne	Cape Washington	1	S 74°38′32″	E 165°25′11″	270
	Baker Rocks	11	S 74°12′38″	E 164°49′39″	177
	Shield Nunatak	50	S 74°33′12″	E 164°30′17″	290
	Edmonson Point	51	S 74°20′00″	E 165°06′25″	355
	Oscar Point	52	S 74°34′57″	E 164°52′29″	57
	Mt. Keineth	74	S 74°29′54″	E 164°08′23″	613
	Markham Island	75	S 74°35′34″	E 164°54′12″	10
	Mt. Melbourne (south)	85	S 74°30′53″	E 164°52′15″	323
	Mt. Melbourne (cone tuff)	113	S 74°19′19″	E 164°38′37″	1790
	Mt. Melbourne (Nunatak)	114	S 74°27′21″	E 164°08′04″	279

structures that show mutual cross-cutting relationships with the major NW–SE strike-slip dextral fault zones. Sinistral strike slip fault zones are often characterised by well-developed damage zones (up-to about thirty centimetre in thickness) and centimetre-thick fault gouges developed at the expense of the volcanic deposits (Fig. 6g).

3.2. Mt. Melbourne area

The volcanic complex of Mt. Melbourne defines a NNE-elongated edifice overlying the Paleozoic basement. The structural architecture in the Mt. Melbourne area includes right-lateral strike-slip fault zones mostly oriented along two main directions: NW–SE (i.e. parallel to the Campbell and Tinker Glaciers) and N–S (i.e. parallel to morphological ridges of Cape Washington) (Fig. 7). Subordinately, E–W right-lateral strike-slip fault zones are also present in the southern part of the edifice (Shield Nunatak and Markham Island). NE–SW-striking extensional fault zones occur in the eastern flank of the volcanic shield (Baker Rocks, Edmonson Point and structural site n° 114). Joint networks show scattered orientations, although the NE–SW and the NW–SE orientations are the most recurrent (Fig. 7). Generally, fault zones consist of distributed, metre-scale spaced and sub-vertical fault surfaces (Fig. 8a, b), often forming decametre-wide (mainly negative) flower structures (Fig. 8b). These fault zones are characterised by well-developed fault-related fracture sets defining metre-thick damage zones. In particular, joint networks are formed by sub-parallel, planar mechanical discontinuities having decametre persistence (Fig. 8c). Spacing of joints systematically decreases from metric to decimetric when approaching the master fault slip surfaces.

In the northern part of the Mt. Melbourne shield, fault zones include (i) discrete conjugate extensional fault zones oriented along NNE–SSW directions (site n° 11), and (ii) dominant dextral strike-slip fault zones along NW–SE directions (site n° 113) (Fig. 7). Above all, NW–SE dextral fault zones are composed by sub-parallel fault strands of hundred metres of length (Fig. 8d,e). The resulting damage zones have fracture-bounded rock lithons, decimetre-to-metre in size, produced by synthetic shear surfaces (Riedel shears) supporting dextral fault kinematics (Fig. 8f).

Volcanic deposits in the southern and eastern sectors of the Mt. Melbourne area show a complex structural pattern (Fig. 7). Dextral strike-slip faults strike from NW–SE (sites n° 1 and 114), to N–S (sites n° 75 and 85), to E–W (sites n° 1, 50, and 75). Dextral strike-slip faults consist of rectilinear fault strands (in plan view) with decimetre thick damage zone and scarce fault core (few millimetre thick along main slip surfaces), and producing centimetre-to-decimetre horizontal displacement (Fig. 8g). At Cape Washington, N–S dextral fault zones cut Pliocene basalts, while E–W ones involve alkali-basaltic lava flows at Markham Island and Shield Nunatak, dated at about 415–430 Ka (Giordano et al., 2012). NE–SW and ENE–WSW sinistral strike-slip fault zones are less persistent and occasionally occur as subsidiary slip surfaces within major dextral strike-slip zones (sites n° 1, 50, and 85). Extensional fault zones strike from WNW–ESE (sites n° 1, 50, 75, and 114) to NE–SW (site n° 1) and show mutual cross-cutting relationships with the dextral strike-slip ones. Planar-to-curvilinear fault strands (in section view) define bookshelf faulting and incipient block rotation cross-cutting the palagonitised lapilli tuffs and the basaltic lava at Markham Island and Shield Nunatak (Fig. 9a–c). WNW–ESE striking extensional fault zones are abundant in the southern portion of the volcano shield. NE–SW striking extensional subsidiary faults are common in the eastern part, from Baker Rocks to Edmonson Point, extending to Oscar Point. They are commonly accompanied by well-developed fault-parallel joints defining metre-thick damage zones. At Oscar Point and Edmonson Point, NE–SW striking joints cut through lapilli tuffs and alkali-basalts, respectively, the latter dated at 120–100 Ka ($^{40}Ar/^{39}Ar$ feldspar dating; Giordano et al., 2012). Finally, low displacement reverse faults strike N–S (site n° 50) and NW–SE (site n° 114) and typically have gentle dip values (less than 20°) and near planar surfaces. The volcanic rocks at the hanging wall of reverse faults are often bent with open-to-isoclinal, inclined-to-recumbent folds (Fig. 9d). At Shield Nunatak (site n° 50), reverse faults truncate and offset (by few tens of centimetre) WNW–ESE extensional fault zones.

4. Discussion

4.1. Regional fault pattern

In the Mt. Overlord area, the structural pattern is rather homogeneous and can be well explained as produced by hundred kilometre-long dextral strike-slip fault system oriented NW–SE, accompanied by subsidiary fault zones having extensional, sinistral, and reverse kinematics (Fig. 10). This pattern fits with a consistent kinematic architecture representative of the state of stress produced by dextral shearing, similar to what described in the near Priestley Glacier (Storti et al., 2006). The inferred brittle regional-scale shear zone corresponds to the trace of the Aviator Fault in Salvini et al. (1997).

In the Mt. Melbourne area, the complex structural pattern is characterised by variable orientations, spatial distributions, and kinematics of the different fault types (Fig. 10). Dextral strike-slip fault zones strike from NW–SE (at north of the volcano) to N–S (towards

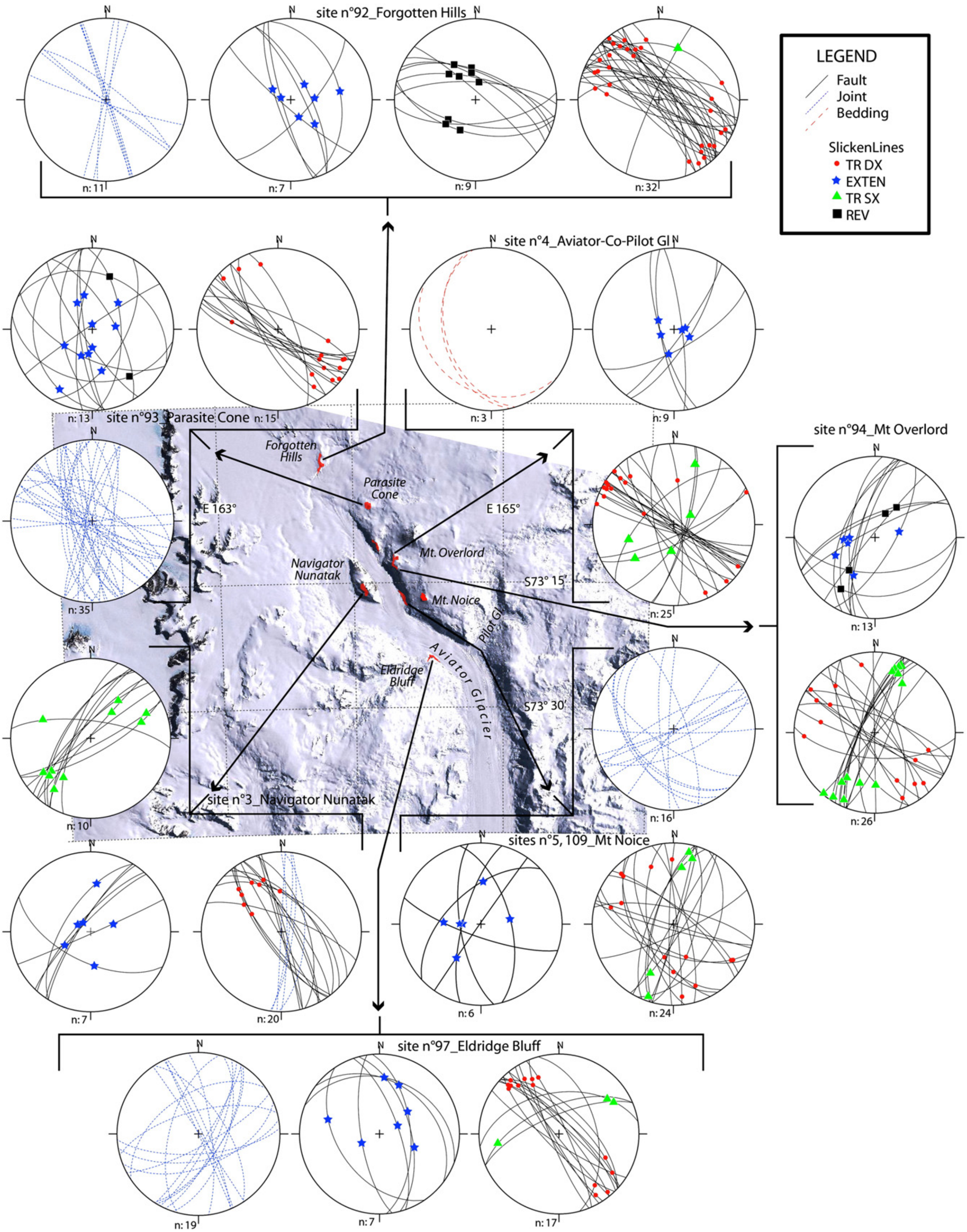

Fig. 4. Landsat image of the area surrounding the Mt. Overlord (Aviator Glacier) where the outcrops of volcanic deposits are shown. Structural data are reported in the stereoplots (Schmidt net, lower hemisphere projection).

the south), to E–W at Shield Nunatak and Markham Island. Extensional fault zones are oriented from NNE–SSW (at Baker Rocks) to WNW–ESE (at the south of the volcano crater, Shield Nunatak and Markham Island). They dislocate dextral shear zones and localise morphological depressions such those at Baker Rocks and Edmonson Point. The structural pattern in the Mt. Melbourne area also includes the local

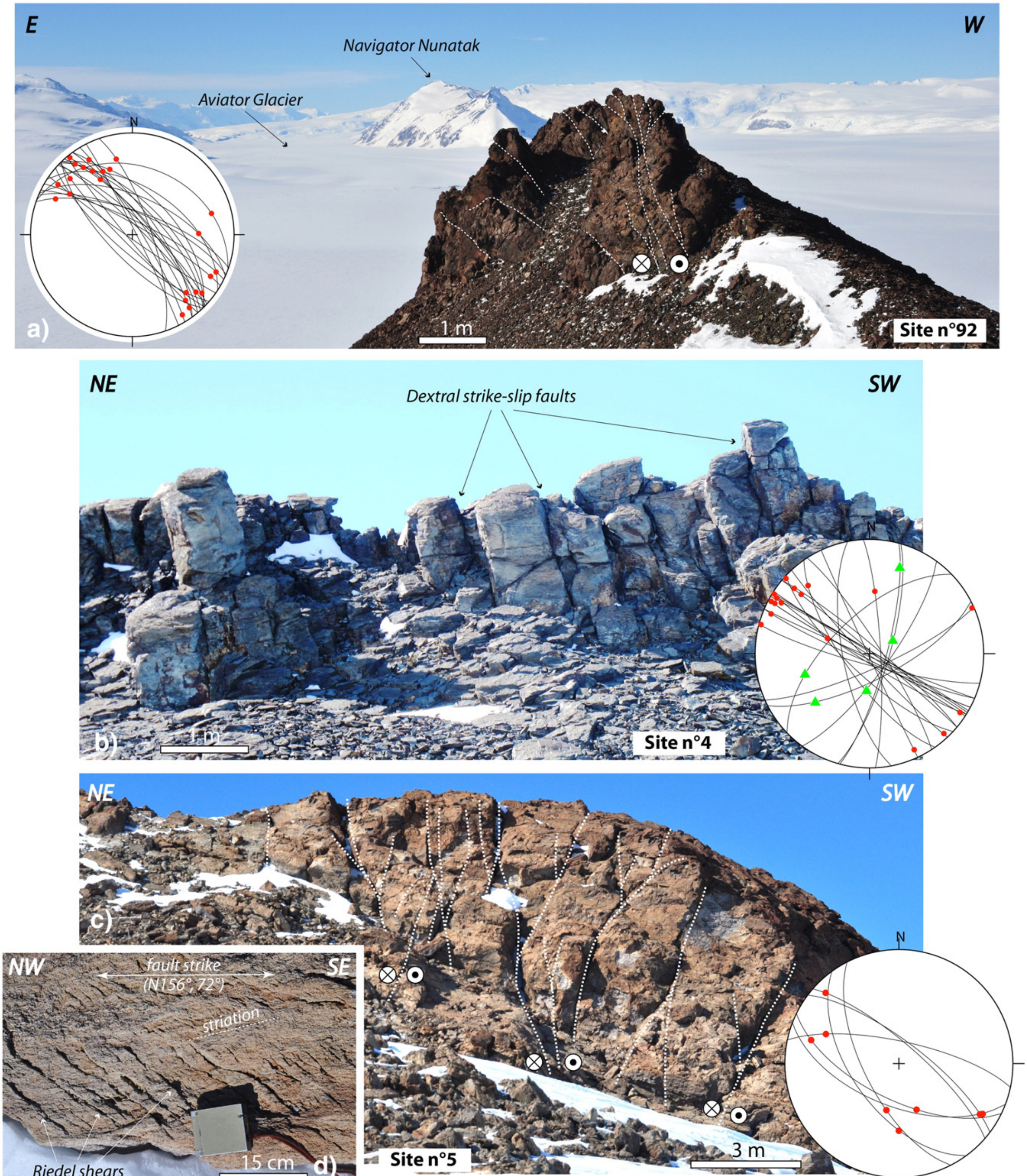

Fig. 5. Fault zones in the Mt. Overlord area. (a) Dolerites at the Forgotten Hills (view to the south towards the Aviator Glacier) involved by metre-spaced fault segments, which are striking NW–SE (see the stereoplot) and are organised in a typical flower structure; (c) half-metre-spaced fault segments affecting foliated dolerite. Faults are dominantly NW–SE dextral strike-slip and subordinate NE–SW sinistral strike-slip (see the stereoplot); (c) massive dolerite affected by diffuse faulting striking NW–SE (Mt. Noice); the stereoplot shows the fault characteristics; (d) detail on a fault surface showing very oblique striations (pitch > 150°) and emergence of synthetic Riedel shears indicating dextral strike-slip kinematics. Refer to Fig. 4 for legend of slickenlines in stereoplots.

occurrence of ~N–S reverse faults that do not show clear evidence of regional significance. The evidence that reverse faulting systematically occurred within larger scale strike-slip fault zones supports their interpretation as second-order structures formed at contractional step-overs and/or by the kinematic stress field generated within the N–S striking strike-slip-dominated fault zone (e.g., Storti et al., 2006). Soft-sediment deformation (producing bending and local shear zones) is a recurrent, but local, effect produced during slumping

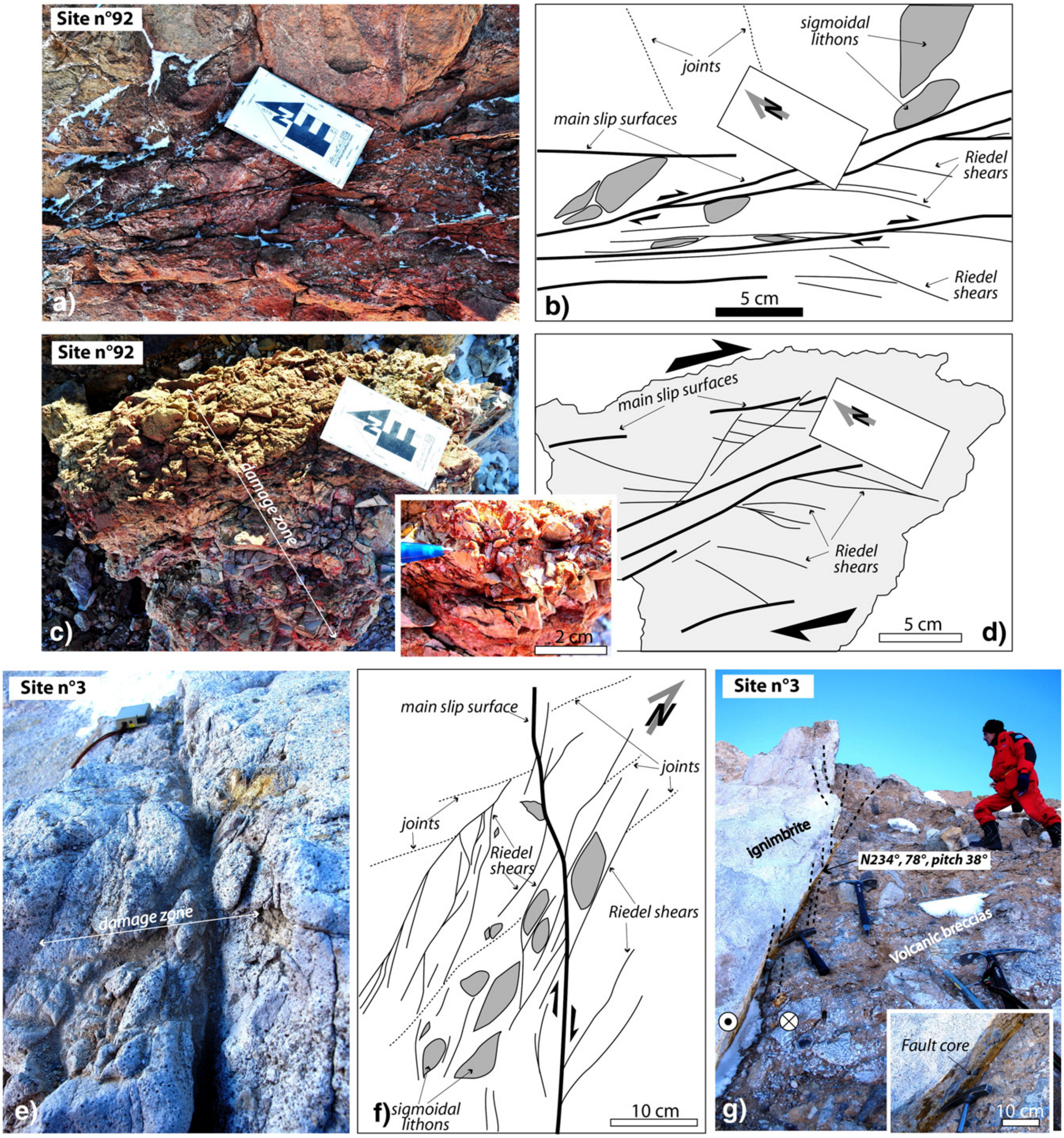

Fig. 6. (a) Plan view a fault zone cutting dolerites at Forgotten Hills. Faulting produced decimetre-thick damage zone provided by main slip surfaces and subordinate synthetic shears (Riedel shears) and tension fractures; (b) line-drawing of picture in (a), interpreting all structures as produced by dextral strike-slip movement; (c) picture and (d) line-drawing of volcanic breccia deformed by the same dextral strike-slip fault zone described above. The inset shows the occurrence of reddish argillic alteration distributed along both major and subordinate deformation features; (e) plan view of a fault zone cutting grey ignimbrite at Navigator Nunatak; (f) line-drawing of (e) showing that the secondary structures accommodating deformation consist of synthetic shears, tension fractures and sigmoidal deformed lithons. All the structures point to a dextral strike-slip movement (pitch is about 32°); (g) sinistral strike-slip fault zone marking the contact with grey ignimbrite and polygenic volcanic breccias at Navigator Nunatak. Note the occurrence of cm-thick fault gouge filled by brownish (argillitic) materials shown in the inset.

mechanisms in sub-glacial hyaloclastites (see also Lanzafame and Villari, 1991).

As a whole, the new data combined with structural datasets collected for the Cenozoic fault network in NVL (Faccenna et al., 2008; Rossetti et al., 2002, 2003, 2006; Storti et al., 2001, 2008) and south Victoria Land (Wilson, 1995; Jones, 1997; Martin and Cooper, 2010) emphasise the dominant role of continental-scale dextral shear zones along the western shoulder of the WARS (Salvini et al., 1997; Storti et al., 2007), where magma ascent and volcanic activity are localised by the NW–SE transtensional tectonic regime (Rocchi et al., 2002, 2003; Salvini and Storti, 1999) rather than a persisting orthogonal extensional scenario (e.g., Davey et al., 2006). In particular, our structural pattern is consistent with evidence of deformation partitioning from dominant NW–SE striking strike-slip fault systems in NVL to a complex, N–S striking fault pattern along the western shoulder of the WARS (Storti et al., 2008), the latter being ascribed to interaction and intersection between pure strike-slip

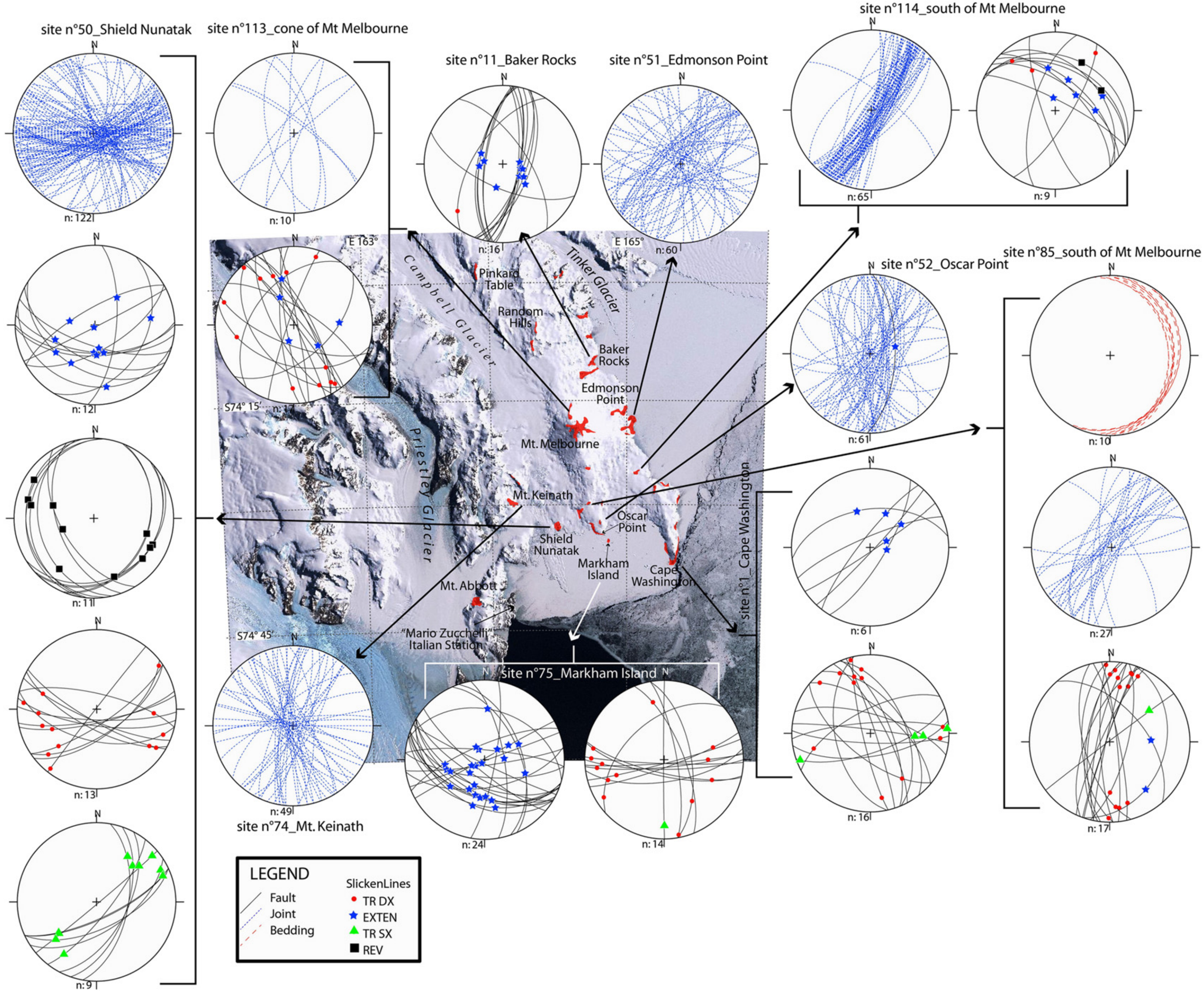

Fig. 7. Landsat image of the area surrounding the Mt. Melbourne and the Campbell and Priestley Glaciers, where the outcrops of volcanic deposits are shown. Structural data are reported in the stereoplots (Schmidt net, lower hemisphere projection).

fault zones and extensional ones (Salvini et al., 1997; Storti et al., 2007). Complex and superimposed structures developing at the tip region of NW–SE dextral intraplate strike-slip fault systems have been proposed as a feasible kinematic scenario for framing the transtensional setting occurring in this area (Storti et al., 2001, 2006, 2007). The accommodation of residual dextral crustal shear is accomplished, in this scenario, by the development of subsidiary structures, where part of the displacement can be transferred (e.g., Kim et al., 2004; Swanson, 1988; Sylvester, 1988).

4.2. Chronology of volcanism and faulting in north Victoria Land

Available geochronological data suggest a rejuvenation of the volcanic activity when moving from the volcanic deposits in the Mt. Overlord (c. 12 Ma; Armienti et al., 1991; Armienti and Baroni, 1999) to the c. 100 ka at the Mt. Melbourne summit crater (Giordano et al., 2012). We use these data for framing the spatio-temporal progression of the structural setting in the study areas and for providing a new picture of Miocene-to-Quaternary faulting during volcanism in NVL (Fig. 11).

Within the Miocene–Pliocene stage (Fig. 11a), the structural pattern in the Mt. Overlord area was defined by the activity of the Aviator NW–SE dextral fault system. Subordinate deformation structures (N–S extensional and NE–SW sinistral strike-slip fault zones) also developed within the NW–SE-oriented regional-scale damage zone associated with the Aviator Fault and contributed to accommodate deformation in both basement and volcanic rocks. Volcanic activity in the Mt. Overlord area was typified by monogenetic edifices distributed along NW–SE transtensional structures, with minor volcanic features (eruptive fissure, cones) aligned along extensional fault zones and tensional fissures (Lanzafame and Villari, 1991). At this stage, the volcanic activity in the Mt. Melbourne area was concentrated in isolated centres in the northern part of the future volcano shield, as suggested by the oldest dated rocks (ca. 12 Ma) at Random Hills and Tinker Glacier (Armienti and Baroni, 1999). To the south, the Miocene–Pliocene period was represented by the formation of the basaltic shield volcano at Cape Washington, dated at 2.7–1.67 Ma (K–Ar whole rock ages; Kreutzer, 1988, unpublished report quoted in Wörner and Viereck, 1989), concurrent with N–S-striking dextral strike-slip faulting.

The Pleistocene–Holocene stage (Fig. 11b) corresponds to a substantial south-eastward migration of the volcanism, possibly associated with enhanced activity in the tip region of the Tinker, Campbell, and Priestley dextral strike-slip fault systems, which created favourable transtensional conditions for localisation of magma emplacement and formation of the Mt. Melbourne volcano. Development of the fault pattern in the Mt. Melbourne area shows correlation with the age of formation of the volcanic features (Giordano et al., 2012). In particular, N–S and E–W transtensional faulting drives the distribution of the oldest peripheral volcanic centres (Cape Washington, Markham Island, Shield Nunatak, Oscar Point) that nucleated south of the present-day summit crater. Conversely, the youngest deposits, dated at Edmonson Point, are affected by NE–SW extensional fault zones, which dissect the older N–S fault set. This suggests that the change in volcanic activity from dispersed centres to the development of the central stratovolcano was associated with a change of the deformation regime during the Quaternary and, in particular, by the activation of major extensional fault zones shaping the modern coastline.

4.3. Implications for active tectonics in Victoria Land

The main fault population affecting the Quaternary volcanic products of the Mt. Melbourne is composed of dominant (i) NW–SE striking dextral strike-slip fault system and (ii) NNE–SSW- and WNW–ESE striking extensional sets. Fault-slip analysis attests that $\sigma3$ (minimum compression) and σ_2 (intermediate compression) paleostress axes are oriented NW–SE and NE–SW, respectively, while the σ_1 (maximum compression) is roughly vertical (Fig. 12a). As such, a general NW–SE stretching direction for the active stress regime in Mt. Melbourne region may be inferred by the cumulative fault population analysis proposed in this study. The inferred stretching direction is sub-parallel to the strike of the main on-shore dextral strike-slip fault systems (i.e. the Tinker, Campbell, Priestley and Aviator faults), and at an oblique angle to the trend of the Transantarctic Mountains.

Quaternary fault arrays arising from structural data collected both in north Victoria Land (Lanzafame and Villari, 1991; Faccenna et al., 2008; this study) and south Victoria Land (Jones, 1997; Martin and Cooper, 2010; Paulsen and Wilson, 2009; Wilson, 1995) show a similar deformation pattern composed by (i) NW–SE dextral strike-slip, (ii) N–S extensional and dextral strike-slip, and (iii) NE–SW extensional and sinistral strike-slip fault zones. The stretching directions provided by the regional fault pattern show, starting from the Admiralty Mountains, a strike near parallel to the trend of the major NW–SE dextral strike-slip fault systems, i.e. oblique to the trend of the Northern Basin and the northern Terror Rift (Fig. 12b). The data to the west of Mt. Melbourne has a peculiar strike, not easy to fit in the first-order kinematic framework and, consequently, it is interpreted to be associated with a “local” case without a regional relevance. To the south, northward of Mt. Morning, the maximum stretching direction strikes near perpendicular to the basin-boundary fault systems of the Ross Sea. At the Mt. Morning and to the east, at the southern tip of the Terror Rift, stretching direction strikes again NW–SE to WNW–ESE.

Overall, this pattern indicates that the dextral transtensional stress regime that initiated in Eocene times (Rossetti et al., 2006) is still responsible for controlling the structural boundary between the Transantarctic Mountains and the WARS (Storti et al., 2007). Nevertheless, the integrated results from Quaternary faulting document an abrupt change in deformation pattern across this structural boundary. To the west, onshore seismicity (Bannister and Kennett, 2002; Reading, 2002) is distributed along the NW–SE striking fault systems connected with the fracture zones and related transform faults in Southern Ocean (e.g., Hayes, 1991; Salvini et al., 1997). To the east, extension controls further development of the offshore fault array that accommodates sedimentation in N–S oriented basins (e.g. Fielding et al., 2008; Salvini et al., 1997). It is intriguing to note that the locus of this change in deformation pattern corresponds to the location of the present-day volcanic activity of the McMurdo Volcanic Group (along the Cape Adare–Mt. Morning alignment), with emplacement of the largest shield volcanoes that reshape the Ross Sea coastline. Furthermore, volcanism seems to localise at the transition from a pure transcurrent regime (on-shore, to the west) to an extensional regime (off-shore, to the east; Salvini and Storti, 1999). This distributed volcanism corresponds, at depth, with a domain of localised high thermal anomaly at the bottom of the continental crust (Danesi and Morelli, 2001; Faccenna et al., 2008). Despite the lack of further geophysical constraints, this thermal anomaly may be advocated to induce perturbation of the rheological state of the

Fig. 8. (a) and (b) Panoramic views to the ignimbrite succession forming two different necks outcropping in the southern flank of the Mt. Melbourne (near the site n° 85). The ignimbrite is pervasively affected by faulting having half-metre-to-metre spacing; note the flower structures in (b); (c) volcanic succession (site n° 114) made by alternation of brownish ash-tuff (up) and volcanoclastic (down) levels severely affected by a joint set striking NE–SW (see the stereoplot) associated with NW–SE dextral strike-slip faulting; (d) picture and (e) line-drawing of the fault zone affecting the volcanoclastic deposit exposed at the base of the sequence shown in (c); note the decrease of the spacing when moving towards east, indicative of the localisation of the main fault surface; (f) detail of a fault surface belonging to the fault zone in (d), showing dextral strike-slip kinematics as deduced from the geometrical intersection between main slip surfaces and Riedel shears; and (g) plan view on a N–S dextral strike-slip fault cutting volcanoclastic levels and producing decimetre horizontal displacement (site n° 85).

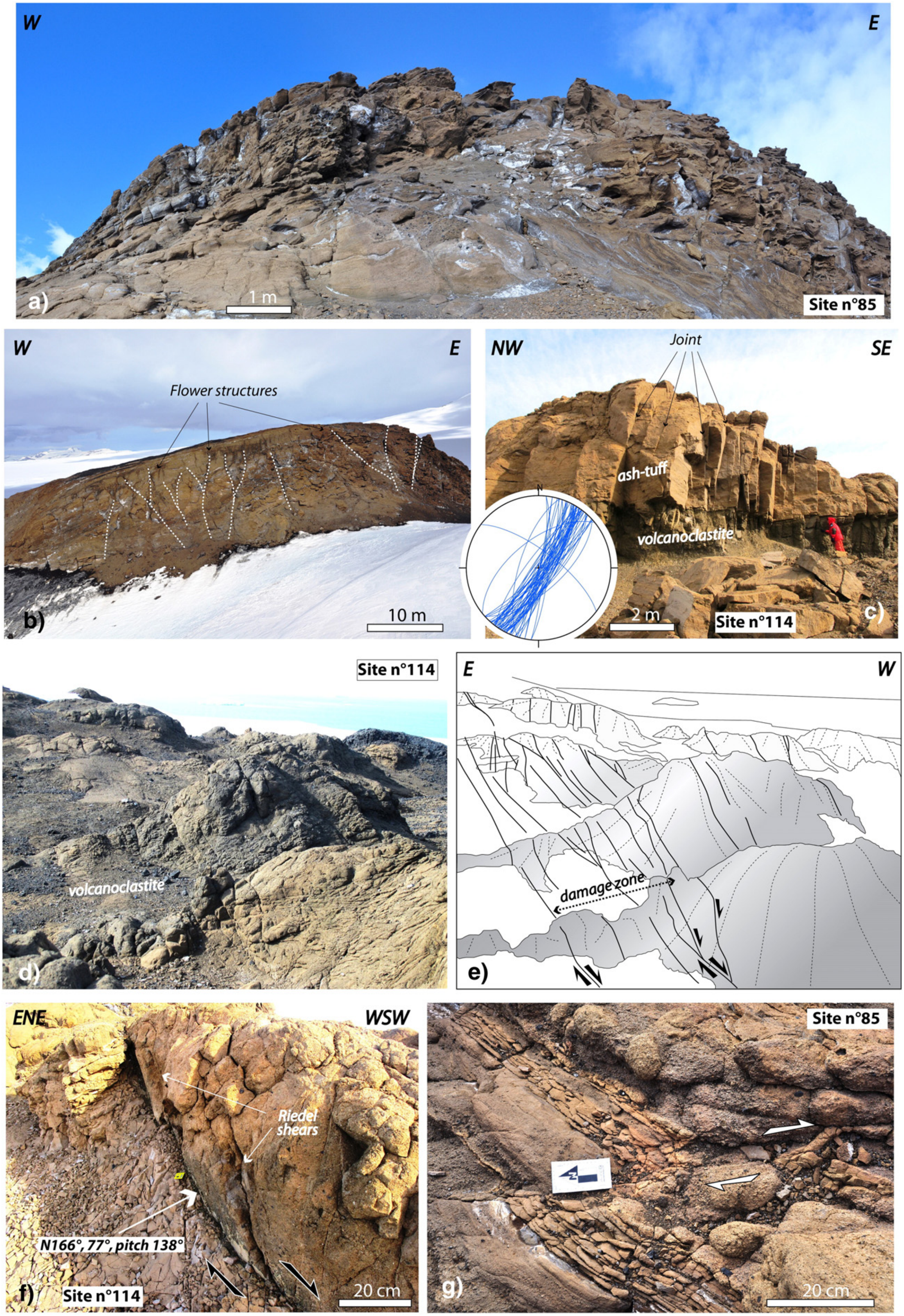
W
E
a)
1 m
Site n°85
W
E
Flower structures
b)
10 m
NW
SE
Joint
ash-tuff
volcanoclastite
N
2 m
Site n°114
c)
Site n°114
volcanoclastite
d)
E
W
damage zone
e)
ENE
WSW
Riedel
shears
N166°, 77°, pitch 138°
f)
Site n°114
20 cm
Site n°85
g)
20 cm

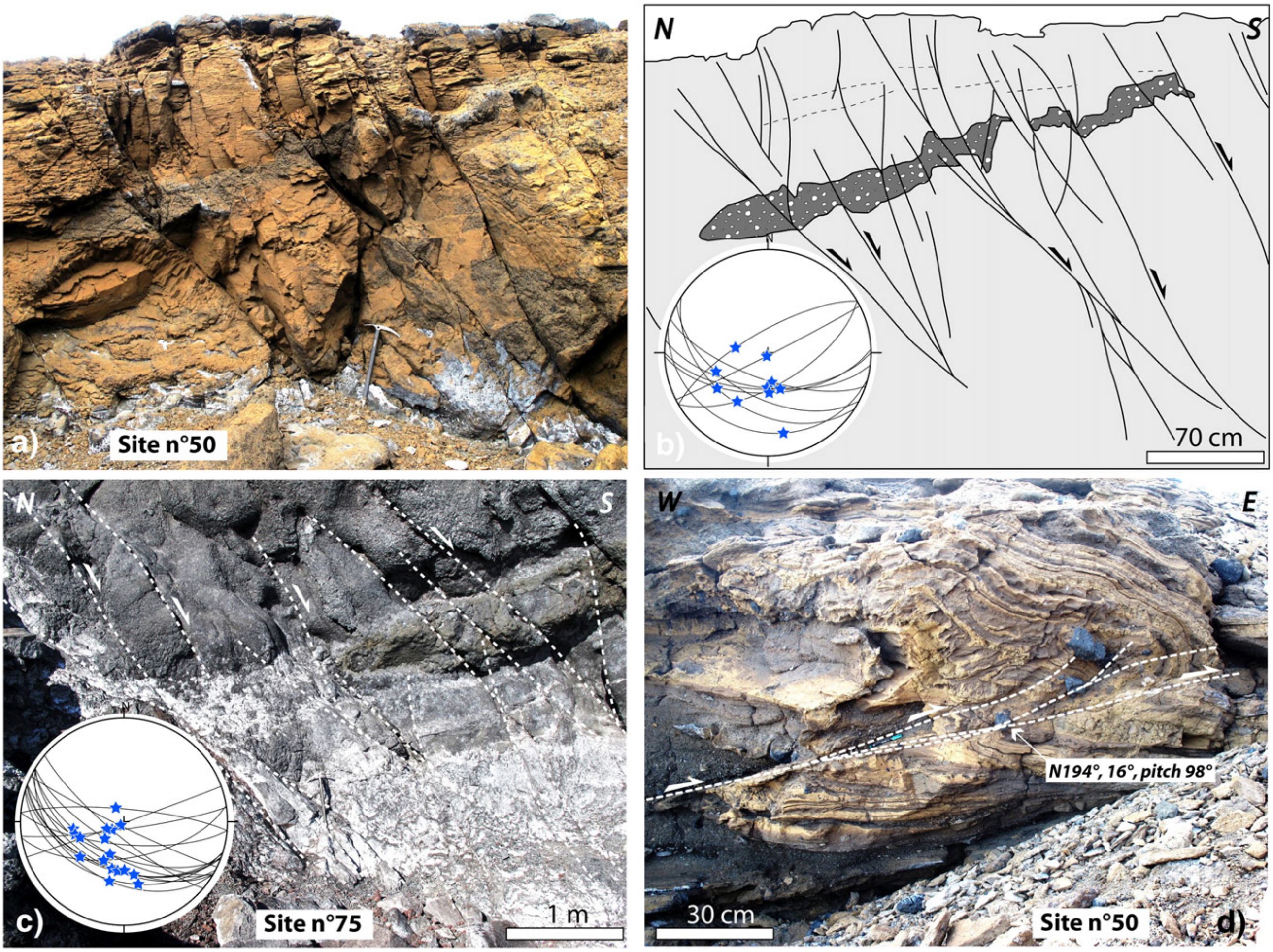

Fig. 9. (a) Ignimbrite at Shield Nunatak (site n° 50) cut by E–W striking extensional faults (see the stereoplot); (b) line-drawing of picture (a) illustrating the geometry and the architecture of the extensional fault zone producing incipient counter-clockwise block rotation; (c) set of metre-spaced, E–W-striking extensional faults (see the stereoplot) affecting the grey volcanoclastites at Markham Island (site n° 75); and (d) N–S striking reverse faults deforming an ignimbrite deposit at Shield Nunatak. Folding of the rocks is associated with faulting. Refer to Fig. 7 for legend of slickenlines in stereoplots.

crust and, in turn, may influence the deformation pattern at the surface during magma emplacement.

5. Conclusions

New structural data from the Mt. Overlord and Mt. Melbourne volcanic systems (McMurdo Volcanic Group), in north Victoria Land, Antarctica, provide evidence for a transtensional stress regime characterising the structural boundary between the Transantarctic Mountains and the West Antarctic Rift System since Miocene times. Particularly, the deformation pattern evolves from NW–SE-striking crustal shear zones having dextral kinematics in the area of the fossil Mt. Overlord volcanic centre, to a more complex transtensional architecture produced by the interference between NW–SE and N–S-striking dextral and N–S-striking extensional fault systems in the area of the active Mt. Melbourne volcano.

Evidence of faulted Quaternary volcanic deposits and fault-controlled morphological features, combined with the spatial distribution of seismic activity, suggests that the tectonics–volcanism coupling being the crustal response to active oblique continental rifting in north Victoria Land. An overall WNW–ESE crustal stretching has been reconstructed for the boundary region between the Transantarctic Mountains and the West Antarctic Rift System, oriented obliquely with respect to the general trend of the belt and the main sedimentary basins, and compatible with an overall oblique rifting scenario.

A major inference from our study is that localisation of active volcanism corresponds to a tectonic environment where the deformation regime changes in space and time (transition from pure transcurrent to extensional regime). Nucleation and propagation of newly-formed segmented faults and fault systems interactions can identify a suitable deformation pattern for migration of magmatic fluids in oblique rifting zones.

Supplementary data to this article can be found online at http://dx.doi.org/10.1016/j.tecto.2015.05.027.

Acknowledgements

This work was supported by the Italian Antarctic Programme (PNRA, grant 2009_ A2.16 (national coordinator: S. Rocchi; local coordinator: F. Storti) and grant Pdr2013/AZ2.07). G.V. and F.B. are warmly grateful for the logistics provided by the PNRA (expedition leader: A. Della Rovere), and acknowledge the helicopter pilots (B. McElhinney and S. Spooner),

Fig. 10. Summary of the main fault (red solid lines) and joint (black dashed lines) patterns observed in the Mt. Overlord and Mt. Melbourne areas (see Table 1). The insets show the conceptual faulting architecture and the orientation of the inferred stress pattern in strike-slip faulting.

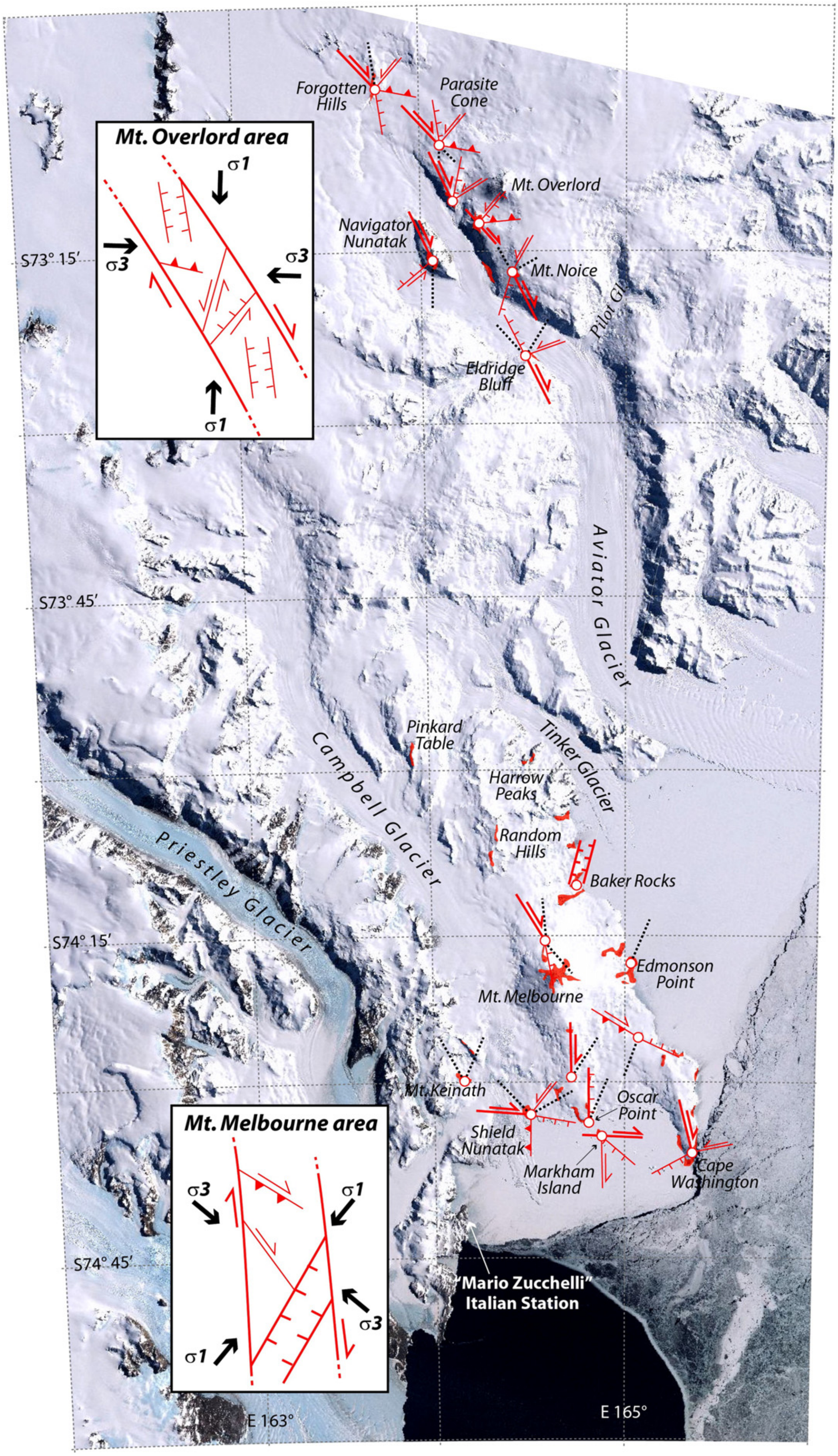
Mt. Overlord area
σ1
σ3
σ3
σ1
Forgotten Hills
Parasite Cone
Mt. Overlord
Navigator Nunatak
S73° 15′
Mt. Noice
Pilot Gl.
Eldridge Bluff
Aviator Glacier
S73° 45′
Pinkard Table
Tinker Glacier
Campbell Glacier
Harrow Peaks
Random Hills
Baker Rocks
Priestley Glacier
S74° 15′
Edmonson Point
Mt. Melbourne
Mt. Keinath
Oscar Point
Shield Nunatak
Markham Island
Cape Washington
Mt. Melbourne area
σ3
σ1
σ3
σ1
S74° 45′
"Mario Zucchelli" Italian Station
E 163°
E 165°

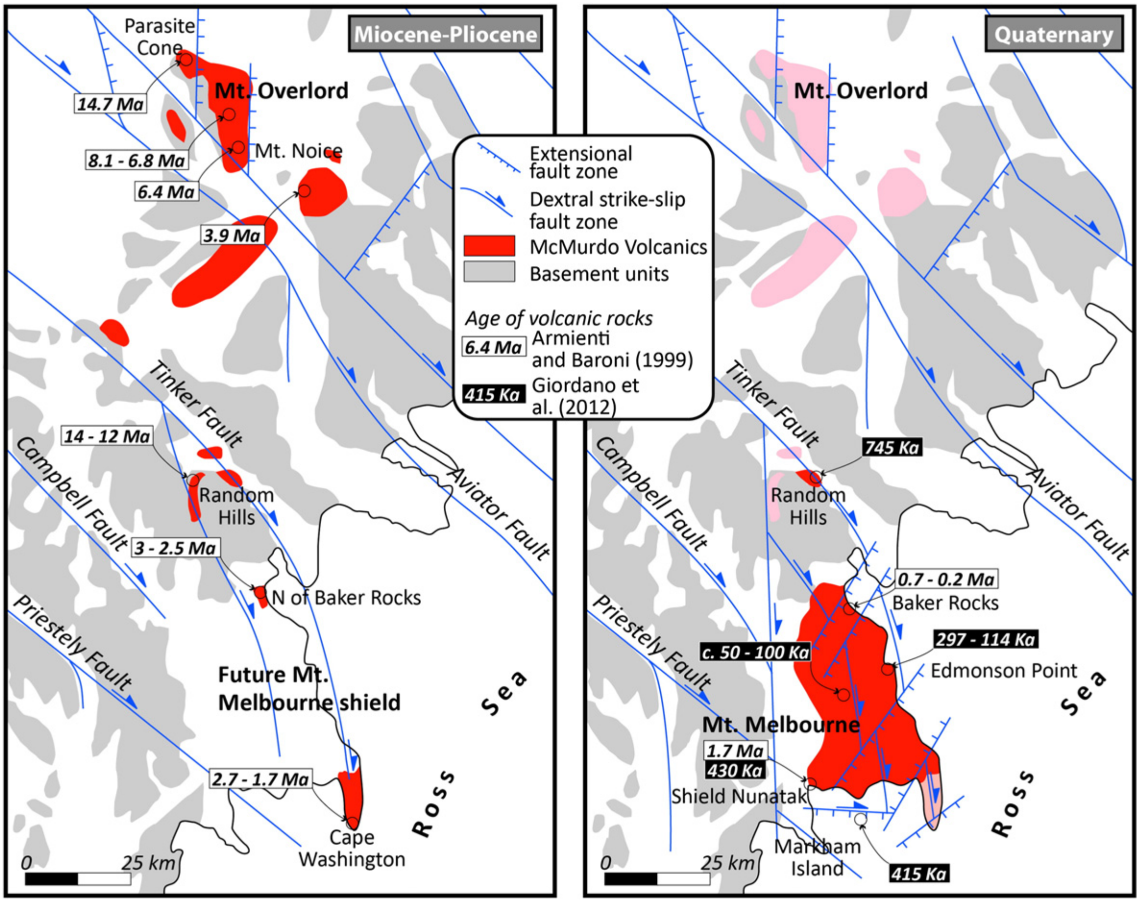

Fig. 11. Two-step schematic sketch for the evolution of the Mt. Overlord–Mt. Melbourne volcanic systems in NVL. Fault patterns are from this study, integrated with data from Storti et al. (2006) and Giordano et al. (2012).

the alpine guides (G. Amort, G. Graziosi, R. Guadagnin), and all colleagues sharing time in the Italian base "Mario Zucchelli". The paper benefited of comments and suggestions by J. Rowland and A Gudmundsson. We also thank the Editor (L. Jolivet) for the manuscript management. This paper is dedicated to the memory of Twin Otter pilot Bob Heath and his crew.

Appendix A1. Quaternary stretching directions of crustal extension in Victoria Land

Here, we summarise the datasets and the geological evidence considered for determining the stretching direction of extension, as schematised in Fig. 12b.

1. Jones (1997). The development of three NE–SW striking Quaternary fault traces in Hidden and Garwood Valleys (South Victoria Land) showing a sinistral strike-slip displacement is attributed to the crustal anisotropy inherited from the Palaeozoic Ross Orogeny. The stretching direction has been extrapolated as reflecting the orientation of the minimum stress axis (σ3) as deduced from the fault kinematic analysis.
2. Martin and Cooper (2010). A set of N–S striking dextral strike-slip faults offsetting a 3.88 ± 0.05 Ma hawaiite dyke from the Mount Morning eruptive centre has been mapped and detailed. The fault system has been interpreted by the authors as the onshore continuation of the West Antarctic rift system (WARS) fault array. The stretching direction has been extrapolated as reflecting the orientation of the minimum stress axis (σ3) as deduced from the fault kinematic analysis.
3. Lanzafame and Villari (1991). In the Mt. Melbourne–Mt. Overlord–Malta Plateau region, the deformation pattern consisting of major structural discontinuities (fault systems and large-throw faults dissecting Holocene terrains) and volcanic features (eruptive fissures and cones) has been reconciled with a coherent framework dominated by NW–SE and NNE–SSW striking extensional structural elements. The stretching direction has been proposed by the authors as deduced from the fault kinematic analysis.
4. Faccenna et al. (2008). The brittle architecture of the Admiralty Mountains, between the Tucker Glacier and the Adare peninsula, has been reconciled with two subsequent episodes of faulting. The second one consists of NE–SW to NNE–SSW striking extensional fault sets associated with the emplacement of large shield alkaline volcanoes from Late Miocene to Present. The stretching direction has been extrapolated as reflecting the orientation of the minimum stress axis (σ3) as deduced from the fault kinematic analysis.
5. Paulsen and Wilson (2009). Several sets of elongate vents and vent alignments on the Mt. Mourning shield volcano (South Victoria Land) have been used for the Pleistocene volcanism along NE trending fissures. The directions of both the maximum (S_H) and minimum (S_h) horizontal stresses have been proposed by the authors. The stretching direction has been considered as reflecting the direction of the minimum (S_h) horizontal stresses, i.e., perpendicular to the fissure trends.

References

Acocella, V., Korme, T., Salvini, F., Funiciello, R., 2002. Elliptic calderas in the Ethiopian Rift: control of pre-existing structures. J. Volcanol. Geotherm. Res. 119, 189–203.

Acocella, V., Porreca, M., Neri, M., Massimi, E., Mattei, M., 2006. Propagation of dikes at Vesuvio (Italy) and the effect of Mt. Somma. Geophys. Res. Lett. 33, L08301. http://dx.doi.org/10.1029/2005GL025590.

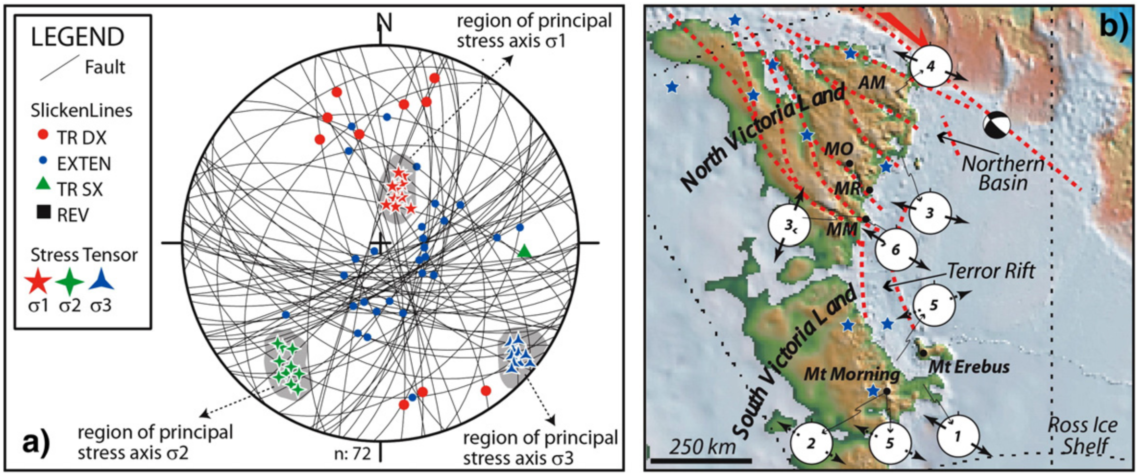

Fig. 12. (a) Cumulative structural data from Quaternary volcanic deposits of the Mt. Melbourne used for reconstructing the orientation of the principal paleo-stress tensors after a Monte Carlo-convergent method; and (b) Structural summary indicating the Quaternary average stretching directions of extension in Victoria Land compared with earthquake locations and available focal mechanisms. Abbreviations: AM: Admiralty Mountains; MM: Mt. Melbourne; MO: Mt. Overlord. Numbers within plot refers to: 1: Jones (1997); 2: Martin and Cooper (2010); 3: Lanzafame and Villari (1991); 4: Faccenna et al. (2008); 5: Paulsen and Wilson (2009); and 6: this study. See Appendix A1 for details on the determination of the stretching direction.

Angelier, J., 1984. Tectonic analysis of fault slip data sets. J. Geophys. Res. 89, 5835–5848.

Angelier, J., 1990. Inversion of field data in fault tectonics to obtain the regional stress. A new rapid direct inversion method by analytical means. Geophys. J. Int. 103, 363–376.

Armienti, P., Baroni, C., 1999. Cenozoic climatic change in Antarctica recorded by volcanic activity and landscape evolution. Geology 27, 617–620.

Armienti, P., Civetta, L., Innocenti, F., Manetti, P., Tripodo, A., Villari, L., De Vita, G., 1991. New petrological and geochemical data on Mt. Melbourne volcanic Field, Northern Victoria Land Antarctica (II Italian Antarctic Expedition). Mem. Soc. Geol. Ital. 46, 397–424.

Atkinson, B.K., 1987. Introduction to fracture mechanics and its geophysical applications. In: Atkinson, B.K. (Ed.), Fracture Mechanics of Rock. Academic Press, London, pp. 1–26.

Bannister, S., Kennett, B.L.N., 2002. Seismic activity in the Transantarctic Mountains — results from a broadband array deployment. Terra Antartica 9, 41–46.

Behrendt, J.C., Lemasurier, W.E., Cooper, A.K., Tessensohn, F., Trehu, A., Damaske, D., 1991. The West Antarctic Rift System: a review of geophysical investigations. Contrib. Antarct.Res. II, Antarct. Res. Ser. 53, 67–112.

Behrendt, J.C., Saltus, R., Damaske, D., McCafferty, A., Finn, C., Blankenship, D.D., Bell, R.E., 1996. Patterns of Late Cenozoic volcanic and tectonic activity in the West Antarctic Rift System revealed by aeromagnetic surveys. Tectonics 15, 660–676.

Bomparola, R.M., Ghezzo, C., Belousova, E., Griffin, W.L., O'Reilly, S.Y., 2007. Resetting of the U–Pb zircon system in Cambro-Ordovician intrusives of the Deep Freeze Range, northern Victoria Land, Antarctica. J. Petrol. 48, 327–364. http://dx.doi.org/10.1093/petrology/egl064.

Buck, W.R., Einarsson, P., Brandsdottir, B., 2006. Tectonic stress and magma chamber size as controls on dyke propagation: constraints from the 1975–1984 Krafla rifting episode. J. Geophys. Res. 111, B12404. http://dx.doi.org/10.1029/2005JB003879.

Caine, J.S., Evans, J.P., Forster, C.B., 1996. Fault zone architecture and permeability structure. Geology 24, 1025–1028.

Cande, S.C., Stock, J.M., Muller, R.D., Ishihara, T., 2000. Cenozoic motion between East and West Antarctica. Nature 404, 145–150.

Capponi, G., Crispini, L., Meccheri, M., 1999. Structural history and tectonic evolution of the boundary between the Wilson and Bowers terranes, Lanterman Range, northern Victoria Land, Antarctica. Tectonophysics 312, 249–266.

Collinson, J.W., Isbell, J.L., Elliot, D.H., Miller, M.F., Miller, J.M.G., 1994. Permian–Triassic Transantarctic basin. In: Veevers, J.J., Powell, C. (Eds.), Permian–Triassic Pangean Basins and Fold Belts along the Panthalassan Margin of Gondwanaland. Geol. Soc. Am. Mem. 184, pp. 173–222.

Danesi, S., Morelli, A., 2001. Structure of the upper mantle under the Antarctic Plate from surface wave tomography. Geophys. Res. Lett. 28, 4395–4398. http://dx.doi.org/10.1029/2001GL013431.

Davey, F.J., Cande, S.C., Stock, J.M., 2006. Extension in the western Ross Sea region-links between Adare Basin and Victoria Land Basin. Geophys. Res. Lett. 33, L20315. http://dx.doi.org/10.1029/2006GL027383.

Di Vincenzo, G., Rocchi, S., Rossetti, F., Storti, F., 2004. ^{40}Ar–^{39}Ar dating of pseudotachylytes: the effect of clast-hosted extraneous argon in Cenozoic fault-generated friction melts from the West Antarctic Rift System. Earth Planet. Sci. Lett. 223, 349–364. http://dx.doi.org/10.1016/j.epsl.2004.04.042.

Di Vincenzo, G., Rossetti, F., Viti, C., Balsamo, F., 2013. Constraining the timing of fault reactivation: Eocene coseismic slip along a Late Ordovician ductile shear zone (northern Victoria Land, Antarctica). Geol. Soc. Am. Bull. 125 (3/4), 609–624. http://dx.doi.org/10.1130/B30670.1.

Dubbini, M., Cianfarra, P., Casula, G., Capra, A., Salvini, F., 2010. Active tectonics in northern Victoria Land (Antarctica) inferred from the integration of GPS data and geologic setting. J. Geophys. Res. 115, B12421. http://dx.doi.org/10.1029/2009JB007123.

Ebinger, C.J., Yemane, T., Woldegabriel, G., Aronson, J.L., Walter, R.C., 1993. Late Eocene–recent volcanism and faulting in the southern main Ethiopian rift. J. Geol. Soc. Lond. 150, 99–108.

Elliot, D.H., Fleming, T.H., 2004. Occurrence and dispersal of magmas in the Jurassic Ferrar large igneous province, Antarctica. Gondwana Res. 7, 223–237.

Faccenna, C., Rossetti, F., Becker, T.W., Danesi, S., Morelli, A., 2008. Recent extension driven by mantle upwelling beneath the Admiralty Mountains (East Antarctica). Tectonics 27, TC4015. http://dx.doi.org/10.1029/2007TC002197.

Faure, G., Mensing, T.M., 2010. The Transantarctic Mountains. Rocks, Ice, Meteorites and Water. Springer http://dx.doi.org/10.1007/978-90-481-9390-5 (832 pp.).

Ferraccioli, F., Armadillo, E., Bozzo, E., Privitera, E., 2000. Magnetics and gravity image tectonic framework of the mount Melbourne volcano area (Antarctica). Phys. Chem. Earth 25, 387–393.

Ferraccioli, F., Armadillo, E., Zunino, A., Bozzo, E., Rocchi, S., Armenti, P., 2009. Magmatic and tectonic patterns over the Northern Victoria Land sector of the Transantarctic Mountains from new aeromagnetic imaging. Tectonophysics 478, 43–61.

Fielding, C.R., Whittaker, J., Henrys, S.A., Wilson, T.J., Naish, T.R., 2008. Seismic facies and stratigraphy of the Cenozoic succession in McMurdo Sound, Antarctica: implications for tectonic, climatic and glacial history. Palaeogeogr. Palaeoclimatol. Palaeoecol. 260, 8–29. http://dx.doi.org/10.1016/j.palaeo.2007.08.016.

Finn, C., Moore, D., Damaske, D., Mackey, T., 1999. Aeromagnetic legacy of Early Palaeozoic subduction along the Pacific margin of Gondwana. Geology 27, 1087–1090.

Fitzgerald, P., 2002. Tectonics and Landscape Evolution of the Antarctic Plate Since the Breakup of Gondwana, with an Emphasis on the West Antarctic Rift system and the Transantarctic Mountains. In: Gamble, J.A., et al. (Eds.), Antarctica at the Close of a Millennium 35. R. Soc. Of N. Z. Bull, Siena, Italy, pp. 453–469.

Flöttmann, T., Gibson, G.M., Kleinschmidt, G., 1993. Structural continuity of the Ross and Delamerian orogens of Antarctica and Australia along the margin of the paleo-Pacific. Geology 21, 319–322. http://dx.doi.org/10.1130/0091-7613(1993)021<0319:SCOTRA>2.3.CO;2.

Giordano, G., Lucci, F., Phillips, D., Cozzupoli, D., Runci, V., 2012. Stratigraphy, geochronology and evolution of the Mt. Melbourne volcanic field (North Victoria Land, Antarctica). Bull. Volcanol. 74, 1985–2005. http://dx.doi.org/10.1007/s00445-012-0643-8.

Goodge, J.W., 2002. From Rodinia to Gondwana: supercontinent evolution in the Transantarctic Mountains. Roy. Soc. NZ Bull. 35, 61–74.

Goodge, J.W., Fanning, C.M., Norman, M.D., Bennett, V.C., 2012. Temporal, isotopic and spatial relations of Early Paleozoic Gondwana-Margin Arc Magmatism, Central Transantarctic Mountains, Antarctica. J. Petrol. 53, 2027–2065.

Granot, R., Cande, S.C., Stock, J.M., Damaske, D., 2013. Revised Eocene–Oligocene kinematics for the West Antarctic rift system. Geophys. Res. Lett. 40, 279–284. http://dx.doi.org/10.1029/2012GL054181.

Gudmundsson, A., 2006. How local stresses control magma-chamber ruptures, dyke injections, and eruptions in composite volcanoes. Earth-Sci. Rev. 79, 1–31.

Gudmundsson, A., 2011. Rock Fractures in Geological Processes. Cambridge University Press (592 pp.).

Gudmundsson, A., Simmenes, T.H., Larsen, B., Philipp, S.L., 2010. Effects of internal structure and local stresses on fracture propagation, deflection, and arrest in fault zones. J. Struct. Geol. 32, 1643–1655.

Hamilton, R.J., Luyendyk, B.P., Sorlien, C.C., Bartek, L.R., 2001. Cenozoic tectonics of the Cape Roberts Rift Basin and Transantarctic Mountain Front, southwestern Ross Sea, Antarctica. Tectonics 20, 325–342.

Harrington, H.J., 1958. Nomenclature of rock units in the Ross Sea Region, Antarctica. Nature 182, 290.

Hart, S.R., Blusztanjn, J., LeMasurier, W.E., Rex, D.C., 1997. Hobbs Coast Cenozoic volcanism: implications for the West Antarctic rift system. Chem. Geol. 139, 223–248.

Hayes, D.E. (Ed.), 1991. Marine Geological and Geophysical Atlas of the Circum-Antarctic to 30° S vol. 54. AGU Antarctic Research Series, Washington, DC.
Jones, S., 1997. Late Quaternary faulting and neotectonics, south Victoria Land, Antarctica. J. Geol. Soc. 153, 645–652.
Kim, Y.S., Peacock, D.C.P., Sanderson, D.J., 2004. Fault damage zones. J. Struct. Geol. 26 (3), 503–517.
Kleinschmidt, G., Tessensohn, F., 1987. Early Paleozoic westward directed subduction at the Pacific margin of Antarctica. In: McKenzie, G.D.M. (Ed.), Gondwana Six: StructureTectonics and Geophysics vol. 4. AGU, Washington, D. C., pp. 89–105.
Kyle, P.R., 1980. Development of heterogeneities in the subcontinental mantle: evidence from the ferrar group, Antarctica. Contrib. Mineral. Petrol. 73, 89–104.
Kyle, P.R., 1990. McMurdo Volcanic Group, Western Ross Embayment. In: LeMasurier, W.E., Thomson, J.W. (Eds.), Volcanoes of the Antarctic Plate and Southern Oceans. Am Geophys Union. Antarctica Research Series 48, pp. 19–145.
Kyle, P.R., Cole, J.W., 1974. Structural control of volcanism in the McMurdo Volcanic Group, Antarctica. Bull. Volcanol. 38, 16–25.
Kyle, P.R., Moore, J.A., Thirlwall, M.F., 1992. Petrologic evolution of anorthoclase phonolite lavas at Mount Erebus, Ross Island, Antarctica. J. Petrol. 33, 849–875.
Lanzafame, G., Villari, L., 1991. Structural evolution and volcanism in Northern Victoria Land (Antarctica): data from Mt. Melbourne–Mt. Overlord–Malta Plateau Region. Mem. Soc. Geol. Ital. 46, 371–381.
Läufer A., Kleindshmidt G., Hejnes-Kunst F., Rossetti F., Faccenna C., 2006. Geological map of the Cape Adare Quadrangle, north Victoria Land, Antarctica, scale 1:250.000. Fed. Inst. for Geosci. and Nat. Resour., Hannover, Germany.
LeMasurier, W.E., 1990. Late Cenozoic Volcanism on the Antarctic Plate: An Overview. In: LeMasurier, W.E., Thomson, J.W. (Eds.), Volcanoes of the Antarctic Plate and Southern OceansAntarct. Res. Ser 48. AGU, Washington, D. C., pp. 1–17.
LeMasurier, W.E., Rex, D.C., 1991. The Marie Byrd Land volcanic province and its relation to the Cainozoic West Antarctic Rift system. In: Tingey, R. (Ed.), The Geology of Antarctica. Oxford Univ. Press, Oxford, UK, pp. 249–284.
LeMasurier, W.E., Thomson, J.W., 1990. Volcanoes of the Antarctic plate and Southern Oceans. Antarct. Res. Ser. 48.
Lesti, C., Giordano, G., Salvini, F., Cas, R., 2008. Volcano tectonic setting of the intraplate, Pliocene–Holocene, Newer Volcanic Province (southeast Australia): role of crustal fracture zones. J. Geophys. Res. 113, B07407. http://dx.doi.org/10.1029/2007JB005110.
Macdonald, K.C., 1998. Linkages Between Faulting, Volcanism, Hydrothermal Activity and Segmentation on Fast Spreading Centers. In: Buck, W.R., Delaney, P.T., Karson, J.A., Lagabrielle, Y. (Eds.), Faulting and Magmatism at Mid-Ocean RidgesAm. Geophys. Union 106. Geophysical Monographies, Washington, DC, pp. 27–58.
Martin, A.P., Cooper, A.F., 2010. Post 3.9 Ma fault activity within the West Antarctic rift system: onshore evidence from Gandalf Ridge, Mount Morning eruptive centre, southern Victoria Land, Antarctica. Antarct. Sci. 22, 513–521. http://dx.doi.org/10.1017/S095410201000026X.
Mouslopoulou, V., Nicol, A., Little, T.A., Walsh, J.J., 2007. Displacement transfer between intersecting regional strike-slip and extensional fault systems. J. Struct. Geol. 29, 100–116.
Müller, R.D., Gohl, K., Cande, S.C., Goncharov, A., Golynsky, A.V., 2007. Eocene to Miocene geometry of the West Antarctic Rift System. Aust. J. Earth Sci. 54, 1033–1045. http://dx.doi.org/10.1080/08120090701615691.
Paulsen, T.S., Wilson, T.J., 2009. Structure and age of volcanic fissures on Mount Morning: a new constraint on Neogene to contemporary stress in the West Antarctic Rift, Southern Victoria Land, Antarctica. Geol. Soc. Am. Bull. http://dx.doi.org/10.1130/B26333.1.
Petit, J.P., 1987. Criteria for the sense of movement on fault surfaces in brittle rocks. J. Struct. Geol. 9, 597–608.
Pollard, D.D., Delaney, P.T., Duffield, W.A., Endo, E.T., Okamura, A.T., 1983. Surface deformation in volcanic rift zones. Tectonophysics 94, 541–584.
Reading, A.M., 2002. Antarctic seismicity and neotectonics. Roy. Soc. NZ Bull. 35, 479–484.
Riley, T.R., Knight, K., 2001. Age of pre-break-up Gondwana magmatism. Antarct. Sci. 13, 99–110.
Rocchi, S., Armenti, P., D'Orazio, M., Tonarini, S., Wijbrans, J., Di Vincenzo, G., 2002. Cenozoic magmatism in the western Ross Embayment: role of mantle plume vs. plate dynamics in the development of the West Antarctic Rift System. J. Geophys. Res. 107 (B9), 2195. http://dx.doi.org/10.1029/2001JB000515.
Rocchi, S., Storti, F., Di Vincenzo, G., Rossetti, F., 2003. Intraplate Strike-Slip Tectonics as an Alternative to Mantle Plume Activity for the Cenozoic Rift Magmatism in the Ross Sea Region, Antarctica. In: Storti, F., Holdsworth, R.E., Salvini, F. (Eds.), Intraplate Strike-Slip Deformation Belts. Geological Society of London Special Publication 210, pp. 145–158.
Rocchi, S., Bracciali, L., Di Vincenzo, G., Gemelli, M., Ghezzo, C., 2011. Arc accretion to the early Paleozoic Antarctic margin of Gondwana in Victoria Land. Gondwana Res. 19, 594–607. http://dx.doi.org/10.1016/j.gr.2010.08.001.
Rossetti, F., Storti, F., Läufer, A., 2002. Brittle architecture of the Lanterman Fault and its impact on the final terrane assembly in North Victoria Land, Antarctica. J. Geol. Soc. Lond. 159, 159–173.
Rossetti, F., Lisker, F., Storti, F., Läufer, A., 2003. Tectonic and denudational history of the Rennick Graben (North Victoria Land): implications for the evolution of rifting between East and West Antarctica. Tectonics 22 (2), 1016. http://dx.doi.org/10.1029/2002TC001416.
Rossetti, F., Storti, F., Busetti, M., Lisker, F., Di Vincenzo, G., Läufer, A., Rocchi, S., Salvini, F., 2006. Eocene initiation of Ross Sea dextral faulting and implications for East Antarctic neotectonics. J. Geol. Soc. Lond. 163, 119–126.
Rossetti, F., Vignaroli, G., Di Vincenzo, G., Gerdes, A., Ghezzo, C., Theye, T., Balsamo, F., 2011. Long-lived orogenic construction along the paleo-Pacific margin of Gondwana (Deep Freeze Range, North Victoria Land, Antarctica). Tectonics 30, TC4008. http://dx.doi.org/10.1029/2010TC002804.
Rowland, J.V., Sibson, R.H., 2004. Structural controls on hydrothermal flow in a segmented rift system, Taupo Volcanic Zone, New Zealand. Geofluids 4, 259–283.
Rowland, J.V., Baker, E., Ebinger, C.J., Keir, D., Kidane, T., Biggs, J., Hayward, N., Wright, T.J., 2007. Fault growth at a nascent slow-spreading ridge: 2005 Dabbahu rifting episode, Afar. Geophys. J. Int. 171, 1226–1246.
Rowland, J.V., Wilson, C.J.N., Gravley, D.M., 2010. Spatial and temporal variations in magma-assisted rifting, Taupo Volcanic Zone, New Zealand. J. Volcanol. Geotherm. Res. 190, 89–108.
Ryan, W.B.F., Carbotte, S.M., Coplan, J.O., O'Hara, S., Melkonian, A., Arko, R., Weissel, R.A., Ferrini, V., Goodwillie, A., Nitsche, F., Bonczkowski, J., Zemsky, R., 2009. Global multi-resolution topography synthesis. Geochem. Geophys. Geosyst. 10, Q03014. http://dx.doi.org/10.1029/2008GC002332.).
Salvini, F., Storti, F., 1999. Cenozoic tectonic lineaments of the Terra Nova Bay region, Ross Embayment, Antarctica. Glob. Planet. Sci. 23, 129–144.
Salvini, F., Brancolini, G., Busetti, M., Storti, F., Mazzarini, F., Coren, F., 1997. Cenozoic geodynamics of the Ross Sea Region, Antarctica: crustal extension, intraplate strike-slip faulting and tectonic inheritance. J. Geophys. Res. 102, 24669–24696.
Salvini, F., Billi, A., Wise, D.U., 1999. Strike-slip fault-propagation cleavage in carbonate rocks: the Mattinata fault zone, Southern Apennines, Italy. J. Struct. Geol. 21, 1731–1749.
Seebeck, H., Nicol, A., Stern, T.A., Bibby, H.M., Stagpoole, V., 2010. Fault controls on the geometry and location of the Okataina Caldera, Taupo Volcanic Zone, New Zealand. J. Volcanol. Geotherm. Res. 190, 136–151.
Storey, B., Leat, P.T., Weaver, S.D., Pankhurst, R.J., Bradshaw, J.D., Kelley, S., 1999. Mantle plumes and Antarctica–New Zealand rifting: evidence from mid-Cretaceous mafic dykes. J. Geol. Soc. Lond. 156, 659–671.
Storti, F., Rossetti, F., Salvini, F., 2001. Structural architecture and displacement accommodation mechanisms at the termination of the Priestley Fault, northern Victoria Land, Antarctica. Tectonophysics 341, 141–161.
Storti, F., Rossetti, F., Läufer, A., Salvini, F., 2006. Consistent kinematic architecture in the damage zones of intraplate strike-slip fault systems in North Victoria Land, Antarctica and implications for fault zone evolution. J. Struct. Geol. 28, 50–63.
Storti, F., Salvini, F., Rossetti, F., Phipps, Morgan J., 2007. Intraplate termination of transform faulting within the Antarctic continent. Earth Planet. Sci. Lett. 260, 115–126.
Storti, F., Balestrieri, M.L., Balsamo, F., Rossetti, F., 2008. Structural and thermochronological constraints to the evolution of the West Antarctic Rift System in central Victoria Land. Tectonics 27, TC4012. http://dx.doi.org/10.1029/2006TC002066.
Swanson, M.T., 1988. Pseudotachylyte-bearing strike-slip duplex structures in the Fort Foster Brittle Zone of southernmost Maine. J. Struct. Geol. 10, 813–828.
Sylvester, A.G., 1988. Strike-slip faults. Geol. Soc. Am. Bull. 100, 1666–1703.
GANOVEX Team, 1987. Geological map of North Victoria Land, Antarctica, 1:500000, Explanatory notes. Geol. Jahrb., B66, 7–79.
Tessensohn, F., Wörner, G., 1991. The Ross Sea rift system, Antarctica: structure, evolution and analogues. In: Thompson, M.R.A., et al. (Eds.), Geological Evolution of Antarctica. Cambridge Univ. Press, New York, pp. 273–277.
Wilson, T.J., 1995. Cenozoic transtension along the Transantarctic Mountains-West Antarctic rift boundary, Southern Victoria Land, Antarctica. Tectonics 14, 531–545.
Wörner, G., 1999. Lithospheric dynamics and mantle sources of alkaline magmatism of the Cenozoic West Antarctic rift system. Glob. Planet. Sci. 23, 61–77.
Wörner, G., Viereck, L., 1989. The Mt. Melbourne volcanic field (Victoria Land, Antarctica). I Field observations. Geol. Jahrb. E38, 369–393.
Wright, T., Ebinger, C.J., Biggs, J., Ayele, A., Yirgu, G., Keir, D., Stork, A., 2006. Magma maintained rift segmentation at continental rupture in the 2005 Afar dyking episode. Nature 422, 291–294.